



Historical Fermi All-sky Variability Analysis of Galactic Flares

S. Joffre¹ , N. Torres-Albà¹ , M. Ajello¹ , D. Kocevski² , and R. Buehler³¹Department of Physics and Astronomy, Clemson University, Kinard Lab of Physics, Clemson, SC 29634, USA²ST12 Astrophysics Branch, NASA Marshall Space Flight Center, Huntsville, AL 35812, USA³Deutsches Elektronen Synchrotron DESY, D-15738 Zeuthen, Germany

Received 2024 February 28; revised 2024 April 19; accepted 2024 April 25; published 2024 June 10

Abstract

The Fermi All-sky Variability Analysis (FAVA) provides a photometric alternative for identifying week-long gamma-ray flares across the entire sky while being independent of any diffuse Galactic or isotropic emission model. We reviewed 779 weeks of Fermi Large Area Telescope data analyzed by FAVA to estimate the rate and origin of Galactic gamma-ray flares, and to search for new variable Galactic gamma-ray transients. We report an estimated yearly rate of ~ 8.5 Galactic gamma-ray flares yr^{-1} , with ~ 1 flare yr^{-1} coming from unknown sources. Out of the known gamma-ray sources that are spatially coincident with these detected flares, we report gamma-ray flares for six of them for the first time. All six are classified as pulsars, or a source of unknown nature but which positionally overlaps with known supernova remnants or pulsar wind nebulae (PWNe). This potentially means these sites are tentative candidates to be the second known site of a variable gamma-ray PWN, after the famous Crab Nebula's PWN. Additionally, we identify nine unassociated flares that are unlikely to have originated from known gamma-ray sources.

Unified Astronomy Thesaurus concepts: Gamma-ray transient sources (1853); Pulsar wind nebulae (2215); Supernova remnants (1667); High mass x-ray binary stars (733); Millisecond pulsars (1062); Pulsars (1306); Gamma-ray astronomy (628); Transient sources (1851); High energy astrophysics (739)

1. Introduction

Launched in June of 2008, the Fermi Gamma-ray Space Telescope regularly surveys the gamma-ray sky with the Large Area Telescope (LAT; Atwood et al. 2009). Fermi-LAT is able to observe the entire sky approximately every 3 hr. This semi-uniform exposure, as well as the LAT's stable instrument response, good angular resolution ($<0.15^\circ$ at >10 GeV), and large energy range (20 MeV–2 TeV) have made Fermi-LAT an ideal instrument for studying time-varying phenomena in the gamma-ray sky.⁴

Ongoing observations by the LAT have shown that the GeV sky is populated by transient sources whose gamma-ray flux varies on an assortment of timescales. Gamma-ray bursts (GRBs) and pulsars' high-energy flux can vary in as short as a fraction of a second (Abdo et al. 2013; Ajello et al. 2019). Day-long flux variations have been observed in the Crab Nebula (Abdo et al. 2010b; Balbo et al. 2011; Striani et al. 2011; Tavani et al. 2011) as well as in multiple novae (Cheung et al. 2016; Li et al. 2017b; Franckowiak et al. 2018; Nelson et al. 2019). Blazars have been observed to emit gamma rays whose emission timescales can vary from days and weeks (Brill 2023; Cutini et al. 2023; Dinesh et al. 2023; Pittori et al. 2023) to months or even years (Abdo et al. 2010c; Nolan et al. 2012; Collaboration 2015; Abdollahi et al. 2020; Peñil et al. 2022; Otero-Santos et al. 2023).

Observations of the transient gamma-ray sky are done across multiple domains and collaborations. Searches for extremely short flares (<1 s) like GRBs are performed on board Fermi, refined on

ground, and made publicly available quickly through the Gamma-ray Coordinates Network (GCN) notices.⁵ Searches of transients on 6 hr to 1 day timescales are performed manually on the ground by the Fermi flare advocates and delivered to the community via Astronomer Telegrams (ATel) and refereed publications (Ciprini & Fermi-LAT Collaboration 2012). Sources whose variability timescale spans from months to years are discovered and published in Fermi-LAT catalogs (Abdo et al. 2010c; Nolan et al. 2012; Collaboration 2015; Abdollahi et al. 2020, 2022). As for flares with a typical duration of 1 week, these have been detected with the Fermi All-sky Variability Analysis (FAVA; Ackermann et al. 2013) and are reported in the first and second catalogs of Flaring Gamma-ray Sources from FAVA (1FAV, Ackermann et al. 2013; 2FAV, Abdollahi et al. 2017).

The vast majority of all the variable sources discovered by Fermi are identified as blazars, a class of extremely variable active galactic nuclei (Urry 1999). The very bright Galactic diffuse emission, which extends up to high Galactic latitudes and all along the Galactic plane, hampers the detection of Galactic transients. Ignorance of the subdegree spatial structure of the Galactic diffuse emission coupled to systematic uncertainty in the LAT instrumental response (both the effective area and the point-spread function, PSF) makes source detection in the plane often difficult on all but the shortest (<1 s) timescales. This has strongly limited our knowledge of Galactic transients. Of the Galactic transients currently detected in gamma rays (excluding pulsars and millisecond pulsars as they are a well-studied population, and their transient nature does not originate from flares), the following Galactic source populations are represented: gamma-ray binaries (Mirabel 2012), novae (Ackermann et al. 2014a), and the Crab Nebula's pulsar wind nebula (PWN; Abdo et al. 2011). However, new detections even within these known source classes are rare.

⁴ Single photon, 68% containment radius.



Original content from this work may be used under the terms of the [Creative Commons Attribution 4.0 licence](https://creativecommons.org/licenses/by/4.0/). Any further distribution of this work must maintain attribution to the author(s) and the title of the work, journal citation and DOI.

⁵ <http://gcnc.gsfc.nasa.gov/ipn.html>

The Incremental Fermi Large Area Telescope Fourth Source Catalog Data Release 4 (4FGL-DR4; Ballet et al. 2023) only reports the firm identifications of 11 binary systems,⁶ eight novae,⁷ and 13 PWNe. If we include associations, the total number of sources represented by these three source classes is 60.⁸ Galactic sources exhibiting transient behavior are even rarer. The 2FAVA (Abdollahi et al. 2017) reports three high-mass binaries (HMBs), five novae, and one PWN (the Crab). The detection of a new Galactic transient has the potential to add significantly to the current data set due to the low statistics of observed Galactic transients.

In this work, we utilized FAVA to identify transients at low latitudes ($|b| < 10^\circ$) that are likely to be of Galactic origin. We define the term “flare” to be a FAVA-detected transient occurring over a week-long period with a positive flux variation. A “long-term flare” is defined to describe any set of spatially coincident FAVA flares that occur in consecutive weeks. We present our method, analysis, and results in the following manner. Section 2 reviews how the positional 95% uncertainty radius ($R_{95\%}$) was calibrated, while Section 3 outlines how FAVA works and our selection criteria for flaring Galactic gamma-ray candidates. Following that, Section 4 outlines the properties of the flares coincident with Galactic gamma-ray sources, as well as with unassociated sources. Lastly, Sections 5 and 6 review and summarize this work.

2. Uncertainty Radius Calibration

Currently, 1FAV and 2FAV include a 0.1° estimated systematic correction factor for a detected flare’s uncertainty radius (Ackermann et al. 2013; Abdollahi et al. 2017). This systematic is based on the positions of known gamma-ray sources in comparison to the detected flares. Additional sources present in the 4FGL enable us to more accurately estimate the systematic uncertainty on a flare’s positional. Following the method discussed at the end of Section 3.1.3 of the 4FGL paper (Abdollahi et al. 2020), we calibrated the maximum-likelihood analysis method’s derived $R_{95\%}$ uncertainty regions for the FAVA-detected gamma-ray flares. First, we cross-matched the FAVA flares that were spatially coincident with a known 4FGL gamma-ray source, giving us 7069 flares. This number reflects the removal of all FAVA detections that reported a $R_{95\%}$ of 0.8° , which is the default value if the maximum-likelihood analysis fails to converge properly. To estimate the systematic uncertainty, we introduce a relative systematic factor, f_{rel} , such that

$$R_{95\text{tot}} = f_{\text{rel}} R_{95\text{stat}}, \quad (1)$$

where $R_{95\text{tot}}$ is the total error (at the 95% confidence level) and $R_{95\text{stat}}$ is the uncertainty error in the position.

Defining Θ as the angular separation between the FAVA-detected source location and the counterpart location of the source, we test various values of f_{rel} until the value y as defined

⁶ The 4FGL identification criterion depends on the source type. For pulsars or X-ray binaries they must find correlated periodic variability to be labeled as a “firm identification.”

⁷ Not all novae detected by Fermi-LAT are reported in the 4FGL-DR4 due to the shorter duration of the flare. Koji Mukai’s running list of all Fermi-LAT-detected novae can be found online: <https://asd.gsfc.nasa.gov/Koji.Mukai/novae/latnovae.html>. As of 2023 June, 18 have been detected.

⁸ A Bayesian (spatial coincidence only) and a likelihood ratio (spatial with log N-log S) method are used for associations. See Section 5 of Abdollahi et al. (2020).

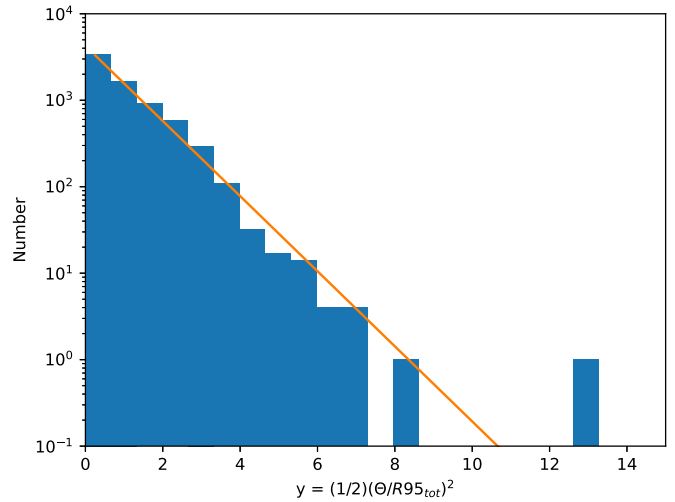


Figure 1. Best fit for calibration of $R_{95\%}$ values with Equation (2) plotted in log-log space; $f_{\text{rel}} = 1.06$.

by

$$y = \frac{1}{2} \left(\frac{\Theta}{R_{95\text{tot}}} \right)^2 \quad (2)$$

follows a Rayleigh distribution (i.e., $\exp(-y)$). Our best fit is achieved for $f_{\text{rel}} = 1.06$, and is plotted in Figure 1. Therefore, all reported $R_{95\%}$ have been increased by 6% over their original values reported by FAVA.

3. Data Selection

All data 2343 procured from the FAVA website.⁹ The last week of data reported in this paper is from week 780 (2023 July 17).

3.1. Fermi All-sky Variability Analysis

The FAVA (Ackermann et al. 2013) identifies transients across the entire sky using a photometric analysis method. In this method, FAVA does not rely on any Galactic diffuse model. Instead, FAVA assumes that the diffuse gamma-ray emission is constant over long time periods ($> \text{weeks}$). FAVA searches for transients by comparing measured counts over a week-long time bin at every point in the sky to the average emission over the first 4 yr of the Fermi mission. FAVA does so while accounting for the difference in exposure time of the sky, and the PSF dependence on both energy and the instrument off-axis angle. Observed counts above this 4 yr averaged emission are analyzed and are converted into a probability of a flare being present. All analysis on the week-long time bins is broken into two energy bands: a low-energy band (LE; 100–800 MeV) and a high-energy band (HE; 800–300,000 MeV). Abdollahi et al. (2017) reports a photometric LE flux sensitivity of $F_{\text{LE}} = 3.67 \times 10^{-7} \text{ cm}^{-2} \text{ s}^{-1}$ and a HE flux sensitivity of $F_{\text{LE}} = 3.24 \times 10^{-8} \text{ cm}^{-2} \text{ s}^{-1}$. To better localize the origin of the flare, a maximum-likelihood analysis is performed at its position. For an in-depth explanation of this and FAVA, please see Abdollahi et al. (2017).

⁹ <https://fermi.gsfc.nasa.gov/ssc/data/access/lat/FAVA/>

Table 1
Cuts on FAVA Data Set for Determining Unassociated Flares

Cut Number	Cut Criterion	Number of Flares Cut	Number of Unassoc. Flares Remaining
1	FAVA weeks 1–780	0	24832
2	$ b < 10^\circ$	22622	2210
3	LE or HE FAVA detection $>5\sigma$	1380	830
4	Unassoc, Unassoc. and Gal. or no 4FGL coincidence	687	143
5	Coincident with 2FAV blazar	12	131
6	WISE IR blazar colors	120	11
7	Solar vicinity	0	11
8	CHIME, BAT, BGM: Gamma-ray burst cross-match	1	10

Notes. See Section 3.2 for a detailed description. For Cut 4, 105 flares are exclusively coincident with a known Galactic 4FGL-DR4 source or a gamma-ray-emitting nova. Ten additional flares are spatially coincident with one or more Galactic 4FGL-DR4 sources or a gamma-ray-emitting nova. All of these flares have a solar distance $>16^\circ$.

3.2. Filter for Identifying Galactic and Unassociated Flare Candidates

To minimize contamination in our data set from extragalactic sources, the following cuts were made. The number of detected flares remaining after the cut is reported. Table 1 gives a summary of the cuts utilized to identify the number of unassociated flaring Galactic gamma-ray candidates. We note that the $R_{95\%}$ used for the FAVA-detected flare is from the localized maximum-likelihood analysis of the flare, where the HE or LE band is used depending on which one is better localized. We have calibrated these $R_{95\%}$ as discussed in Section 2.

1. All detected flares from the FAVA website from week 1 to week 780¹⁰ (2008 August 4–2023 July 17) at a threshold of >5 ¹¹ are downloaded (this equals 24,832 flares).¹²
2. All flares with a Galactic latitude $|b| < 10^\circ$ are retained (2210 flares remain).
3. Only flares whose low-energy and/or high-energy FAVA detection is at least 5σ are saved (this leaves 830 flares remaining).
4. The remaining flares are then positionally cross-matched with the 4FGL-DR4 (Ballet et al. 2023), Roma-BZCAT (Massaro et al. 2015), as well as the list of definitive gamma-ray-emitting novae by Koji Mukai.¹³ We break this down into four categories:
 - (a) Flares positionally coincident with a 4FGL-DR4 blazar or a blazar reported in the Roma-BZCAT. These flares are removed.
 - (b) Flares exclusively coincident with the position of a known 4FGL-DR4 Galactic source or a gamma-ray-emitting novae (i.e., are not spatially coincident with an unassociated or known blazar source). These flares

are set aside and are categorized as originating from known Galactic sources.

- (c) Flares positionally coincident with a 4FGL-DR4 unassociated source, or with a 4FGL-DR4 unassociated source and a known Galactic source.
- (d) Flares that do not positionally coincide with a gamma-ray source reported in the 4FGL-DR4.

The 4FGL-DR4 does not provide gamma-ray $R_{95\%}$ for some of the detected novae, as well as not detecting others, hence why we utilize the compiled gamma-ray novae list. This second subset (flares exclusively coincident with the position of a known 4FGL-DR4 Galactic source or a gamma-ray-emitting novae) is composed of 105 individually unique FAVA flares. This subset is set aside and will be discussed at the end of this section. The last two items encompass possibly new or unknown sources, and are the subset of flares we discuss for the remainder of the data selection cuts (143 flares).

5. Flares that are coincident with a 2FAV source that is associated with a known blazar are eliminated (131 flares remain).
6. Following the Wide-Field Infrared Survey Explorer (WISE) blazar strip as reported in Massaro et al. (2012), we developed a code to filter out any flare detection whose $R_{95\%}$ contains a WISE source (from the AllWISE catalog) with infrared colors within the blazar strip in all three-dimensions (W1–W2 versus W2–W3, W2–W3 versus W3–W4, and W1–W2 versus W3–W4) as this is considered a likely blazar.¹⁴ Upper limits on reported AllWISE magnitudes are considered (11 flares remain).
7. FAVA reports the real-time angular distance of the flare to the position of the Sun at the time the flare was detected. Following Ackermann et al. (2013), since the Sun is a bright gamma-ray-emitting source, we cut all flares whose Sun distance is less than 12° . None of these remaining flares met this criteria, so none were cut (11 flares remain).
8. Lastly, in order to see if the unassociated FAVA-detected flares are coincident with other transient detections, we cross-matched our remaining flares with the First Chime/

¹⁰ Week 768 is excluded due to analysis complications from the FAVA pipeline so the data are not accessible.

¹¹ This is not equivalent to a 5σ Gaussian significance. See the GitHub page for notes.

¹² See <https://github.com/dankocevski/pyFAVA> and the Appendix for more details.

¹³ Included in the downloadable files for this paper.

¹⁴ See https://github.com/tryingastronomy/Blazar_codes/tree/main/AW_blazar_strip and the Appendix for more details.

FRB Fast Radio Burst catalog (CHIME/FRB Collaboration et al. 2021), the Swift/BAT Hard X-Ray Transient Monitor (Krimm et al. 2013), the Third Swift Burst Alert Telescope (BAT) Gamma-Ray Burst (GRB) Catalog (Lien et al. 2016), the Fourth Fermi-GBM Gamma-Ray Burst Catalog (von Kienlin et al. 2020), and the Fermi-LAT catalog of long-term gamma-ray transient sources (1FLT; Baldini et al. 2021). The only spatial cross-matches that occur is with the Third Swift-BAT GRB Catalog and the Fourth Fermi-GBM Gamma-Ray Burst Catalog. Both catalogs report the detection of GRB 221009A (R.A., decl.: 288.26, 19.77; 2022 October 9 at 13:16:58.99 UTC; Lesage et al. 2023), which is both spatially and temporally coincident with one of the 11 remaining unassociated FAVA flares (flare 7401). This GRB is the recently detected brightest-of-all-time (or BOAT) GRB with the highest total isotropic-equivalent energy and highest fluence and peak flux GRB ever identified (Burns et al. 2023). Therefore, this flare is removed (10 flares remain).

9. Flares that have coincident positions based on overlapping $R_{95\%}$ are assumed to be flaring events likely originating from the same source. Only two of the 10 unassociated flares spatially overlap (see Table 5). We thus report nine unique, new flaring objects of unknown origin.

Over almost 15 yr of data, we find a total of nine distinctly new flaring sources (composed of 10 flares) that have not been associated to any known gamma-ray-detected source and are of potential Galactic origin (see Table 5). We find an additional 105 flares that are coincident with a single Galactic gamma-ray source, plus 10 flares that are coincident with more than one, resulting in a total of 115 flares coincident with at least one Galactic gamma-ray source (see Table 2). This means we have 125 flares of likely Galactic origin. Section 5.1 discusses the yearly flare rate more thoroughly.

The flares that are spatially associated with Galactic gamma-ray sources, novae, and unassociated flares are all outlined in three separate tables. Table 2 reports on nonnovae concomitant with FAVA detections, Table 3 reports on the FAVA detections of classical novae, and Table 5 reports on FAVA flares that we propose as originating from unidentified Galactic transient sources.

3.3. Rate of Spurious FAVA Detections

Since we are selecting flares on a 5σ statistical significance, this leaves a margin for spurious detections. To evaluate the likelihood of one of our FAVA-detected flares being spurious, we first calculate the total number of trials. The number of trials can be calculated using

$$N_{\text{trials}} = N_{\text{weeks}} \times N_{\text{channels}} \times N_{\text{sky pixels}}, \quad (3)$$

where N_{trials} , N_{weeks} , N_{channels} , and $N_{\text{sky pixels}}$ all correspond to the number of trials, weeks, energy channels, and sky pixels used in the analysis, respectively. With $N_{\text{weeks}} = 779$, $N_{\text{channels}} = 2$, and $N_{\text{sky pixels}} = 165,012$, where

$$N_{\text{sky pixels}} = \frac{\text{Total Sky}}{\text{Pixel}} = \frac{41,253 \text{ deg}^2}{0.25 \text{ deg}^2} = 165,012, \quad (4)$$

resulting in $N_{\text{trials}} = 257,088,696$. Since a 5σ detection corresponds to a probability $P = 3 \times 10^{-7}$, this means there

is a one in 3,333,333 chance of a wrongful detection. Dividing our number of trials by 3,333,333, we expect 77 spurious FAVA detections out of 257,088,696 trials. From our 779 weeks analyzed, we find 13,218 flares were detected at a 5σ level, meaning we expect 0.5% of all FAVA detections to be false. Hence, we do not expect any of our vetted flares to be of spurious origin.

3.4. Background Extragalactic Contamination Estimates

Ackermann et al. (2013) found that by simulating extragalactic sources at low latitudes (after accounting for differences in solid angle and sensitivity corrections), 60% of low-latitude, variable extragalactic sources would be able to be detected by LAT. The 2FAV also reports a total of 323 flares at $|b| < 10^\circ$, of which 249 are associated to an extragalactic source. We therefore anticipate that of the 2210 flares our investigation finds at $|b| < 10^\circ$, 1701 are likely of extragalactic origin. After all of our cuts that were implemented to eliminate extragalactic contamination, we removed over 2000 flares (with 125 Galactic gamma-ray flare candidates remaining). The number of removed flares means it is very likely that we have properly accounted for this potential contamination on a statistical basis.

3.5. Robustness of the 3D Wide-Field Infrared Survey Explorer Blazar Strip

Filter criterion No. 6 in Section 3.2, the 3D WISE Blazar strip (W1–W2, W2–W3, W3–W4; Massaro et al. 2012), was tested using (i) 4FGL-DR4 blazars, (ii) 4FGL-DR4 Galactic sources, and (iii) known Fermi-LAT-detected gamma-ray novae

3.5.1. Testing Known Blazar Sources

The 4FGL-DR4 contains 3934 blazars of the BL Lacertae, flat-spectrum radio quasar, and undetermined type. In this catalog, the gamma-ray detection is reported as well as the associated counterpart, if known. Using the $R_{95\%}$ of the 4FGL-DR4 gamma-ray detection, we verify whether or not a WISE source contained therein has WISE colors that would place it within all three dimensions of the blazar strip. Of the 3934 known blazars in the 4FGL-DR4, $\sim 96\%$ are compatible (considering the upper limits) with the blazar strip.

Of the known blazars, $\sim 89\%$ are at high latitude ($|b| > 10^\circ$). This leaves 420 known blazars at a latitude of $|b| < 10^\circ$. Of the blazars that lie in the plane, $\sim 76\%$ are captured in all three dimensions of the blazar strip.

3.5.2. Testing Known Galactic Sources as Reported by 4FGL-DR4

The 4FGL-DR4 reports 584 sources of Galactic origin (pulsars, SNRs, HMBs, etc.). Of the reported Galactic sources, 405 occur at low latitudes ($|b| < 10^\circ$). Of the known Galactic sources at low latitude (as some are at $|b| > 10^\circ$), $\sim 39\%$ have uncertainty regions which contain a WISE source whose colors are consistent with a blazar. This means our method wrongly captures $\sim 39\%$ of low-latitude Galactic sources as blazars. Many of these WISE sources report upper limits (i.e., the value of the magnitude is a minimum) for the different WISE filters. If one of the WISE source's color values has the possibility to fall in the blazar strip because of this limit, we count it as a possible blazar.

Table 2
DR4 Galactic Sources Coincident with FAVA Galactic Flare Candidates^f

Associated Source	4FGL Name	DR4 Source Class ^a	LE σ^k	HE σ^k	Exclusive Flare Number ^b	Max Possible Flare Number ^c	$\Gamma_{4\text{FGL}}^d$	$\Gamma_{LE\text{avg}}^e$	$\Gamma_{HE\text{avg}}^e$
Cygnus X-3	4FGL J2032.4+4056	HMB	11.89	4.78	30	36	-2.68 ± 0.04^h	-2.52 ± 0.22	-2.56 ± 0.52
Crab Nebula (IC Field)	4FGL J0534.5+2201	PWN	23.56	4.29	28	...	N/A ^{h,i}	-3.38 ± 0.34	-2.26 ± 0.73
PSR B1259–63	4FGL J1302.9-6349	HMB	18.41	6.84	21	...	-2.33 ± 0.27	-2.83 ± 0.20	-2.17 ± 0.69
LS I +61 303	4FGL J0240.5+6113	HMB	7.08	2.49	7	8	-2.39 ± 0.005^h	-2.33 ± 0.27	-1.85 ± 0.64
PSR J0248+6021	4FGL J0248.4+6021	PSR	6.29	1.07	3	4	-2.64 ± 0.02^j	-2.96 ± 0.33	-3.01 ± 0.59
PSR J2032+4127	4FGL 2032.2+4127	PSR	8.51	3.97	2	8	-2.61 ± 0.01^j	-2.61 ± 0.19	-2.73 ± 0.56
PSR J1731–1847	4FGL J1731.7-1850	msp	5.01	−0.46	1	...	-2.65 ± 0.09^h	DNC ^l	DNC ^l
SNR G016.0–00.5 ^f	4FGL J1821.4-1516	spp	5.55	4.03	1	...	-2.90 ± 0.09^h	-2.96 ± 0.32	-0.06 ± 0.78
SNR G016.7+00.1 ^f	4FGL J1821.1-1422	spp	5.55	4.03	-2.66 ± 0.06^h
PSR J1826–1256 ^g	4FGL J1826.1-1256	PSR	9.66	1.04	1	...	-2.46 ± 0.01^j	-2.14 ± 0.28	-1.59 ± 0.54
SNR G018.1–00.1 ^g	4FGL J1824.1-1304	spp	9.66	1.04	-2.94 ± 0.09^h

Notes.

^a Capitalized classifications are confirmed associations, lowercase are positionally coincident associations: high-mass binary (HMB), pulsar wind nebula (PWN), pulsar (PSR), nova (NOV), millisecond pulsar (msp), or potential association with supernova remnant or pulsar wind nebula (spp).

^b Number of FAVA flares that are spatially coincident with only this Galactic source and no others.

^c Total possible number of FAVA flares that could have originated from this Galactic source, where we include flares that are coincident with this and at least one other DR4 known Galactic source. “...” corresponds to the maximum number being the same as the Exclusively Coincident Flare Number.

^d 4FGL-DR4 reported power-law photon index.

^e Average photon index of all FAVA flares exclusively coincident with the source listed.

^f These Galactic sources are spatially coincident with the same flare, FID 3472.

^g These Galactic sources are spatially coincident with the same flare, FID 3473. Two additional unassociated 4FGL sources are also coincident with the edge of the flare: 4FGL J1826.5-1202c and 4FGL J1828.1-1312.

^h 4FGL-DR4 best fit as LogParabola.

ⁱ 4FGL-DR4 does not report a power-law fit for the inverse-Compton emission of the Crab PWN. It is fit with a LogParabola model with LP_Index=1.75 and LP_beta=0.08.

^j 4FGL-DR4 best fit as PLSuperExpCutoff.

^k Highest detection recorded. Note, may not be the same flare for the LE σ and HE σ columns.

^l Follow-up maximum-likelihood analysis did not converge (DNC).

Table 3
Gamma-Ray Novae Coincident with FAVA Galactic Flare Candidates

Name	Date of Gamma-Ray Peak ^a Y/M/D	Paper/ATel	Ang. Sep ^b (deg)	FAVA $R_{95\%}$ ^c (deg)	FAVA Dates of Detection Y/M/D	FIDs ^d	LE σ	HE σ	Γ_{LE}	Γ_{HE}
V407 Cyg	2010/3/13-14	Abdo et al. (2010a)	0.12	0.08	2010/3/11-22	843,853,862	5.64 ^e	10.27 ^e	-1.37 ± 0.25^e	-2.52 ± 0.20^e
V959 Mon	2012/06/22-6/24	Cheung et al. (2012b)	0.06	0.16	2012/6/18-25	2033	7.39	8.27	-1.82 ± 0.23	-3.33 ± 0.43
V1324 Sco	2012/6/15-7/2	Cheung et al. (2012a)	0.06	0.07	2012/6/18-25	2034	4.15	6.43	-1.17 ± 0.33	-2.54 ± 0.24
V339 Del	2013/08/16	Hays et al. (2013)	0.07	0.08	2013/8/12-19	26314, 26423	8.73 ^e	10.76 ^e	-1.25 ± 0.22^e	-2.54 ± 0.24^e
V5855 Sgr	2016/10/28-11/1	Li & Chomiuk (2016)	0.31	0.80	2016/10/31-11/7	4311	4.71	5.22	DNC	DNC
V5856 Sgr	2016/11/8	Li et al. (2016)	0.22	0.80	2016/11/7-14	43231	6.82	14.64	DNC	DNC
V906 Car	2018/4/10-4/14	Aydi et al. (2020)	0.09	0.04	2018/4/16-30	5071,5082	19.05 ^e	24.76 ^e	-1.81 ± 0.09^e	-2.62 ± 0.09^e
V392 Per	2018/4/30-5/8	Albert et al. (2022)	0.04	0.07	2018/4/20-5/7	5091	4.55	6.38	-0.55 ± 0.76	-2.19 ± 0.22

Notes. Table 3.

^a Date as given by corresponding paper or ATel.

^b Average angular separation between the optically detected novae location and the FAVA-detected flare. Rounded up to hundreths of degree.

^c If multiple flares, the best (smallest) localized $R_{95\%}$ is reported.

^d Bolded text indicates the FID corresponding to the most significant detection (in both bands).

^e Corresponds to the flare of highest significance.

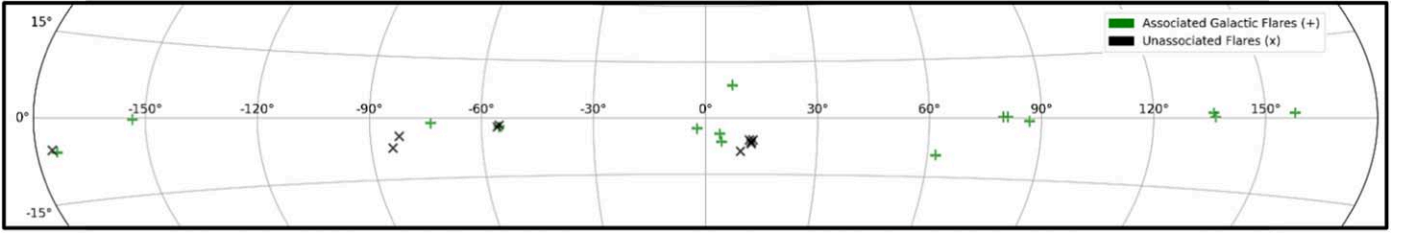


Figure 2. Sky distribution of detected flares. A single exclusively coincident FAVA flare that is spatially associated with a Galactic gamma-ray source or nova from Tables 2 and 3 is represented by one of the 15 green crosses (as four sources are nonexclusive with the spatially coincident flare their flares are not included). The 10 black ‘X’s correspond to the 10 unassociated Galactic flare candidates in Table 5.

3.5.3. Fermi-LAT Detected Gamma-Ray Novae

We also test Koji Mukai’s compiled list of Fermi-LAT-detected classical novae mentioned in the introduction (Section 1). Of the 18 definitive detections (reported as of 2023 October 10), only 10 have a WISE source within $5''$ of the optically detected location. Out of these 10 sources, only one falls in all three blazar strips (V407 Cyg, which we detect with FAVA; see Table 3). Since we assume that the lack of a WISE source means that the source in question is not a blazar, then we only mistake gamma-ray novae for blazars 6% of the time.

3.5.4. Sensitivity and Specificity of 3D WISE Blazar Strip

Since we are particularly interested in this test working at low latitudes ($|b| < 10^\circ$) we report the results of low-latitude sources reported in the 4FGL-DR4. For clarification:

1. True positives (TPs) are low-latitude blazars flagged as blazars.
2. False positives (FPs) are low-latitude Galactic sources flagged as blazars.
3. True negatives (TNs) are low-latitude Galactic sources which have no WISE sources in their $R_{95\%}$ with colors consistent with blazars in all three dimensions of the WISE blazar strip. Therefore, these are not flagged by the blazar strip (because they are not blazars).
4. False negatives (FNs) are low-latitude blazars whose $R_{95\%}$ contains no WISE source with colors consistent with a blazar in all three dimensions of the WISE blazar strip. Therefore, this blazar is not flagged by the blazar strip as a blazar.

Sensitivity, or true-positive rate (TPR), is defined as

$$\text{TPR} = \frac{\text{TP}}{\text{TP} + \text{FN}}, \quad (5)$$

while specificity, or true-negative rate (TNR), is defined by

$$\text{TNR} = \frac{\text{TN}}{\text{TN} + \text{FP}}. \quad (6)$$

For our purposes, sensitivity reflects the ability of the test to correctly identify a source as a blazar. Specificity, on the other hand, reflects the ability of the test to identify nonblazar sources (i.e., Galactic sources). From the tests in Sections 3.5.1 and 3.5.2, we find the following values:

1. TP = 318 blazars flagged as blazars.
2. FP = 159 Galactic sources flagged as blazars.
3. TN = 246 Galactic sources not flagged as blazars.
4. FN = 102 blazars not flagged as blazars.

This results in a sensitivity (or TPR) of 75.7% and a specificity (TNR) of 60.7%. These values can be combined to determine the test accuracy (ACC):

$$\text{ACC} = \frac{\text{TP} + \text{TN}}{\text{TP} + \text{TN} + \text{FP} + \text{FN}}, \quad (7)$$

which, when the above values are evaluated in Equation (7), the result is $\text{ACC} = 68.4\%$. The accuracy value reflects the fraction of blazars and Galactic sources which are properly flagged compared to the entire set that is analyzed.

4. Results

4.1. Overview of FAVA Flare Properties Coincident with Galactic Sources

We find 115 FAVA-detected flares that are spatially coincident with at least one 4FGL Galactic gamma-ray source, with 105 flares exclusively coincident (spatially) with a single Galactic source. We have determined that all 115 flares spatially coincide with only 19 known Galactic gamma-ray sources. Approximately $\sim 75\%$ of the 105 flares that are spatially coincident with a single Galactic gamma-ray source can be attributed to Cygnus X-3, the Crab Nebula, and the HMB system of PSR B1259–63. See Section 4.3 for more discussion. The distribution of the location of origin of these flares on the sky is depicted in Figure 2. Overall, the source types that are spatially coincident with a FAVA flare are as follows: high-mass binary (HMB), pulsar wind nebula (PWN), pulsar (PSR), nova (NOV), millisecond pulsar (msp), and potential association with supernova remnant or pulsar wind nebula (spp).

The sources reported in Table 2 are typically best fit with a LogParabola model in the 4FGL-DR4, but for the sake of comparison with the FAVA fits, we only report the power-law fit for each source from the 4FGL. Additionally, we report the averaged FAVA LE and FAVA HE band indices from the FAVA-detected flares that are spatially coincident with the 4FGL source. Out of the known Galactic sources detected by FAVA, the hardest spectrum reported by the DR4 is PSR B1259–63, with $\Gamma_{4FGL} = -2.33 \pm 0.27$. The hardest LE band source is the PSR J1826–1256 or SNR G018.1–00.1 at -2.14 ± 0.28 . Of flares spatially coinciding with a 4FGL Galactic source, the only flare detected at a $>5\sigma$ level in the HE band is PSR B1259–63.

Among the 18 known gamma-ray novae so far, using our selection criteria, eight were detected by FAVA (see Table 3). These are V407 Cyg, V959 Mon, V1324 Sco, V339 Del, V5855 Sgr, V5856 Sgr, V906 Car, and V392 Per. Two of these novae had FAVA flares that were coincident with other sources. Flare Identification number (FID) 862, which we have

identified as V407 Cyg, is also positionally coincident with SNR G085.9–00.6. But, due to the temporal coincidence during the height of the gamma-ray emission from V407 Cyg (see Abdo et al. 2010a), this flare most likely originated from the nova. Similarly, FID 4311 encompasses the positions of both V5855 Sgr and the blazar of uncertain type (bcu) NVSS J181120–275946. The Variability_Index (VI; as reported by the 4FGL-DR4) of this blazar is 16.27, which falls below the threshold (27.69) at which the source has a 99% chance of being variable. This flare is detected in the same week that V5855 Sgr peaked in gamma rays (Li & Chomiuk 2016; Li et al. 2016; Munari et al. 2017). We therefore conclude that this flare originated from V5855 Sgr.

Selecting the most significant detections from the novae with multiple detections, six novae were detected above 5σ in both LE and HE bins, while the remaining three were detected only in the HE bin (see Table 3). No gamma-ray-detected nova flares were detected exclusively in the LE bin. The average LE photon index of all of these novae is $\Gamma_{\text{LE}} = -1.49 \pm 0.39$, while the average HE photon index is $\Gamma_{\text{HE}} = -2.57 \pm 0.36$. The stark difference in slope between the LE and HE bin (being hard and soft, respectively) points to these novae emission peaking between the two bins. Since the dividing line is at 800 MeV, we expect that many of these gamma-ray-detected novae are displaying a cutoff around a few GeV, which has been reported in previous analyses (Ackermann et al. 2014b; Metzger et al. 2016).

4.2. Associated Galactic Sources Detected by FAVA with Previous Flaring Behavior

In the following subsections, we outline our findings of flaring behavior for the number of sources previously known to vary that are spatially coincident with FAVA flares. Furthermore, we outline the previously understood flaring nature of these sources. We reiterate that the term “flare” is meant to be a FAVA-detected flare occurring over a week-long period unless otherwise noted. A “long-term” flare is meant to describe any set of spatially coincident FAVA flares that occur in consecutive weeks. For visualization of these source’s variability, Appendix B contains the Fermi Light Curve Repository (LCR; Abdollahi et al. 2023) light curves over the course of the Fermi mission. Time is binned in week-long intervals.

4.2.1. Cygnus X-3

In this investigation, we report 30 FAVA flares exclusively coincident (spatially) with this source, and six additional flares that are also coincident with PSR J2032+4127. Further, we find Cygnus X-3 to have the highest number of coincident FAVA-detected flares out of any known Galactic gamma-ray source. Of these 30 week-long flares, 10 occur in 2020 while nine occur in 2021, with a total of seven long-term flares.

Cygnus X-3 is a HMB and the first microquasar detected by Fermi-LAT (Fermi LAT Collaboration et al. 2009). Composed of a neutron star or black hole (Koljonen & Maccarone 2017), this is one of the few binaries of this type where the donor star is a Wolf–Rayet star (van Kerkwijk et al. 1992). Furthermore, the Fermi LAT Collaboration et al. (2009) found Cygnus X-3 to have a 4.8 hr orbital period. Recent work done by Prokhorov & Moraghan (2022) used a variable-size sliding-time-window

analysis to detect 23 intervals of 28 days windows where Cygnus X-3’s gamma-ray emission was detected at levels $>4\sigma$.

In 2021, four FAVA-detected flares occur consecutively, from 2021 May 17 to 2021 June 14, likely detecting a single long-term flare. We find that in 2020, the 10 flares do not happen all consecutively, with the longest long-term flare happening from 2020 August 24 to 2020 September 14 (3 weeks). Prokhorov & Moraghan (2022) also reports a single long-term flare between 2020 April 27 and 2020 September 14. Lastly, Prokhorov & Moraghan (2022) reports the detection of a long-term flare from Cygnus X-3 during 2020 September 14–2021 August 12. FAVA detects 11 (nonconsecutive) flares during this time.

4.2.2. Crab Nebula (Pulsar Wind Nebula)

Coming in second for the most FAVA flares spatially coincident with a Galactic gamma-ray source, this investigation reports 28 spatially coincident FAVA flares with the Crab Nebula. Long-term flares are detected three times.

One of the most well-studied gamma-ray sources on the sky, the Crab is composed of a pulsar at its center surrounded by a nebula and the scattered remains of the supernova that occurred in 1054 A.D. (Minkowski 1942). Even before the first FAVA catalog paper (Ackermann et al. 2013), gamma-ray flares from the Crab Nebula had been observed (Abdo et al. 2011; Tavani et al. 2011; Buehler et al. 2012). Abdo et al. (2011) identified a 16 days flare and 4 days flare in 2009 February and 2010 September, respectively. Later, Striani et al. (2013) proposed the transient gamma-ray nature of the Crab to come from flares (above-average flux on the order of hours) and “waves” (above-average outbursts occurring on the order of 1–2 weeks), the latter being formed by plasma instabilities with enhanced magnetic fields. Striani et al. (2013) records seven different wave events from AGILE and Fermi-LAT data, one of which corresponds to one of our 28 FAVA flares that are exclusively coincident with the Crab. Labeled W6 in Striani et al. (2013), this wave-natured flare is reported to have lasted 12 days from 2012 March 2 to 2012 March 14. The temporally coincident FAVA detection occurred in the week from 2012 March 5 to 2012 March 12.

4.2.3. PSR B1259–63

We find 21 FAVA flares to be exclusively coincident with the HMB system PSR B1259–63, with all flares being part of four individual long-term flares.

PSR B1259–63 is a pulsar that is part of a HMB system, with a massive B2e or Oe star companion (Wang et al. 2004; Aharonian et al. 2005; H.E.S.S. Collaboration et al. 2020). This source has a well-reported orbital period of ~ 1237 days, with an eccentricity of $e = 0.87$ (Wang et al. 2004). Prior to and after periastron, PSR B1259–63 traverses the disk-like outflow of its partner star, with the disruption causing emission from radio to TeV energies. See Johnson et al. (2018) for a robust description of the system. The crossings were observed by Fermi-LAT, with the gamma-ray emission typically peaking ~ 40 –60 days after periastron in 2010 (Abdo et al. 2011; Tam et al. 2011), 2014 (Caliandro et al. 2015), 2017 (Chang et al. 2018; Johnson et al. 2018; Tam et al. 2018), and 2021 (Chernyakova et al. 2021). The official dates for the previous periastrons of this source are reported as 2010 December 14

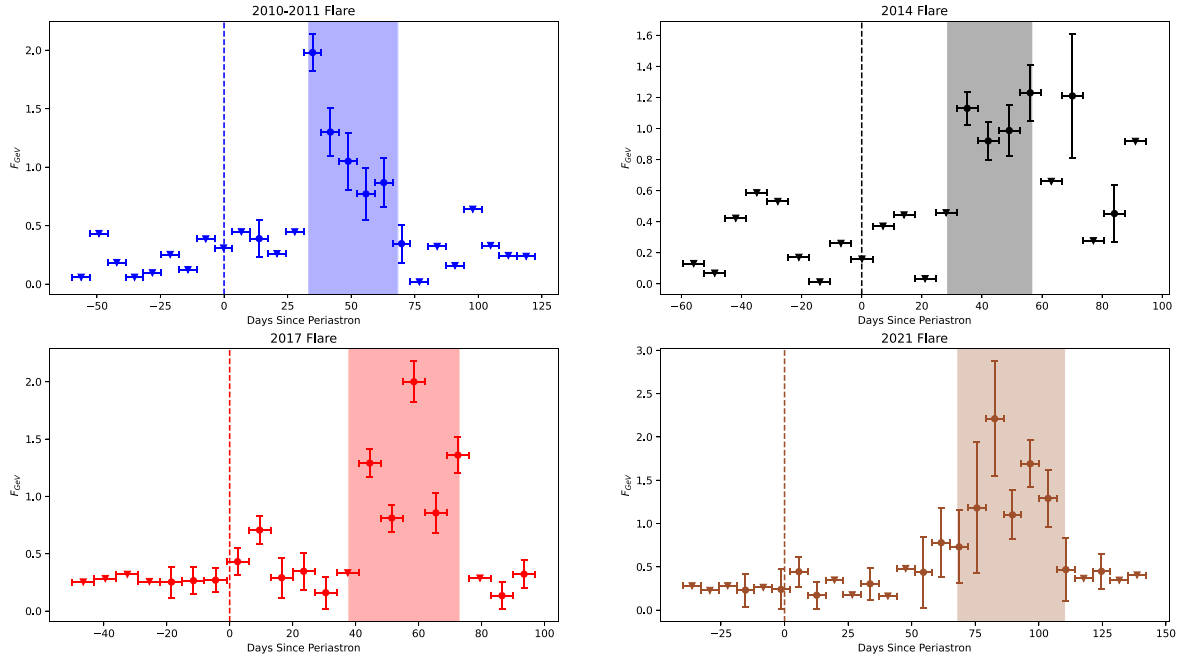


Figure 3. Adapted from Figure 1 in Chernyakova et al. (2021). F_{GeV} is the Fermi-LAT-detected photon flux for $E > 100$ MeV in units of 10^{-6} photons $\text{cm}^{-2} \text{s}^{-1}$ plotted against the number of days since periastron of PSR 1259-63. The dashed vertical line indicates point of periastron and highlighted regions are the consecutive weeks in which FAVA detected a significant long-term flare spatially coincident with this source.

16:39:03 UTC, 2014 May 4 10:02:22 UTC, 2017 September 22 03:25:41, and 2021 February 9 20:48:59 UTC.

The 21 flares detected by FAVA that are exclusively coincident with this source follow the delayed gamma-ray emission of the disk crossing. The gamma-ray flares detected by FAVA in multi-week epochs are as follows: two 5 week long-term flares (2011 January 17–2011 February 21 and 2017 October 30–2017 December 4), one 4 week long-term flare (2014 June 2–2014 June 30), and one 7 week long-term flare (2021 April 19–2021 May 31). Figure 3 is adapted from Chernyakova et al. (2021), which plots the Fermi-LAT flux over time. We have added highlighted bands indicating the consecutive weeks of detection by FAVA. Overall, FAVA accurately captures the peak gamma-ray emission as detected by Fermi-LAT.

Prokhorov & Moraghan (2022) also reports multi-week flaring behavior of PSR B1259-63 in gamma rays, with a 5 week detection starting on 2017 October 25, and therefore overlapping with one of the long-term FAVA detections of this source.

4.2.4. LS I +61 303

LS I +61 303 is coincident with seven flares exclusively, with no detections in consecutive weeks.

LS I +61 303 is another HMB system, with either a black hole or neutron star and a large Be star. One of the first sources whose orbital periodicity was detected in gamma rays, LS I +61 303 has a 26.6 ± 0.5 day orbital period (Abdo et al. 2009). Others propose that LS I +61 303 could be a magnetar (see Torres et al. 2011; Suvorov & Glampedakis 2022). Nonetheless, the object is known to be transient in gamma rays. FAVA only detected this source on seven occasions, and only in the 2009–2019 decade (but not in consecutive weeks).

4.3. Associated Galactic Sources Detected by FAVA with No Previous Flaring Behavior

This section focuses on sources that we report to be flaring in gamma rays for the first time. In each case, a Galactic gamma-ray source with no known history of gamma-ray flaring behavior was found to be positionally coincident with at least one of the FAVA-detected flares. These sources are PSR J0248+6021, PSR J2032+4127, PSR J1731-1847, SNR G016.0-00.5, SNR G016.7+00.1, PSR J1826-1256, and SNR G018.1-00.1.

4.3.1. PSR J0248+6021

Our investigation finds a total of four flares coincident with the pulsar PSR J0248+6021, three of which are solely coincident with this source. Although Theureau et al. (2011) detected a series of short bursts above the average signal strength of the pulsar, these bursts occurred in radio frequencies and on time periods analogous to the pulsar’s spin period of 217 ms.

The First Large High Altitude Air Shower Observatory (LHAASO) is a TeV air-shower detector composed of a Water Cherenkov Detector Array (WCDA) and the Kilometer Squared Array (KM2A; Cao et al. 2024). The First LHAASO Catalog of Gamma-ray Sources (1LHAASO) reports persistent TeV sources. LHAASO’s WCDA data came from 2021 March 5 to 2022 September 30, while KM2A detections are reported from 2020 January to 2020 September. Two of the three FAVA-detected flares exclusively coincident with this pulsar occurred in weeks during the time period of the 1LHAASO catalog. Although the 4FGL-DR4 does not report a TeV flag from previous TeV telescopes, both LHAASO detectors report a TeV source coincident with PSR J0248+6021. The significance of these detections is reported with the Test Statistic (TS) where the TS is defined as $TS = 2\ln(L/L_0)$ where L is the maximum likelihood for a source being present, while L_0 is the maximum

likelihood for the null hypothesis (Cao et al. 2024). 1LHAASO J0249+6022 is detected by KM2A (R.A., decl.: 42.39, 60.37; $R_{95\text{ stat}} = 0.40^\circ$, $\Gamma_{\text{KM2A}} = 3.82 \pm 0.18$) with a significance, of $\text{TS} = 148.8$ and by WCDA (R.A., decl.: 41.52, 60.49; $R_{95\text{ stat}} = 0.16^\circ$, $\Gamma_{\text{WCDA}} = 2.52 \pm 0.16$) at $\text{TS} = 53.3$. The position of these sources in comparison to PSR J0248+6021 is seen in Figure 4. We note that $\Gamma_{4\text{fgl}}$, Γ_{LEavg} , and Γ_{HEavg} all are in agreement with Γ_{WCDA} within 1σ (see Table 2).

1LHAASO proposes that the TeV source corresponds to an astrophysical system associated with PSR J0248+6021 (e.g., a composite SNR). Therefore, we propose that our FAVA-detected flares are the first week-long detected gamma-ray outbursts involving PSR J0248+6021 and a neighboring system, or nearby feature such as a nebula.

4.3.2. PSR J2032+4127

In 2017, the pulsar PSR J2032+4127 was identified to be in a binary system with a $15 M_\odot$ star (Ho et al. 2017), with the pulsar displaying X-ray brightening (Ho et al. 2017). Li et al. (2017a) conducted long-term X-ray observations and found week-long variability embedded in the long-term increasing trend. Li et al. (2018) conducted studies with Fermi-LAT but did not detect variability at GeV energies.

Due to the vicinity of a nearby TeV source, Abeysekara et al. (2018) used the Major Atmospheric Gamma Imaging Cherenkov telescope (MAGIC; Bigongiari 2005) and the Very Energetic Radiation Imaging Telescope Array (VERITAS; Holder et al. 2006) to observe PSR J2032+4127, in which they detected gamma-ray emission rising to a factor of 10 above baseline before quickly dropping off a week later. These results led PSR J2032+4127 to be the second TeV gamma-ray binary system to be detected with the compact object nature known. Abeysekara et al. (2018) model the low state and high state of the outburst as a power law plus a baseline component. The MAGIC detection of the outburst has a best fit of $\Gamma_{\text{MAGIC low}} = 2.57 \pm 0.26$ and $\Gamma_{\text{MAGIC high}} = 2.17 \pm 0.23$, with the low-state index agreeing with the LE and HE average indices detected by FAVA (see Table 2). These MAGIC/VERITAS observations occurred during periastron (2017 November 13) and do not correspond with the coincident FAVA flares.

The pulsar PSR J2032+4127 is spatially coincident with eight FAVA flares (see Table 2). Two of these flares (FIDs 6012 and 6911) are exclusively coincident with PSR J2032+4127, meaning that they are spatially coincident with only this gamma-ray source and no other. The other six flares are spatially coincident with both PSR J2032+4127 and Cygnus X-3 (which is known to flare; see Section 4.2.1). It is possible that some of these flares originate from Cygnus X-3, but identifying the origin of these flares requires further analysis. As for the origin of FIDs 6012 and 6911, the Fermi LCR (Abdollahi et al. 2023) reports a heightened flare state in weekly time bins for Cygnus X-3 during both of these flares. Therefore, we find it likely that these originate from Cygnus X-3. Even so, there are many potential locations for high-energy radiation and particle acceleration within the vicinity of this field, and the lack of simultaneous TeV and GeV flares does not discount the potential for MeV or GeV flares to originate from this pulsar environment. Furthermore, the FAVA-detected flares are not well localized enough to determine the point of origin. If any of these FAVA-detected

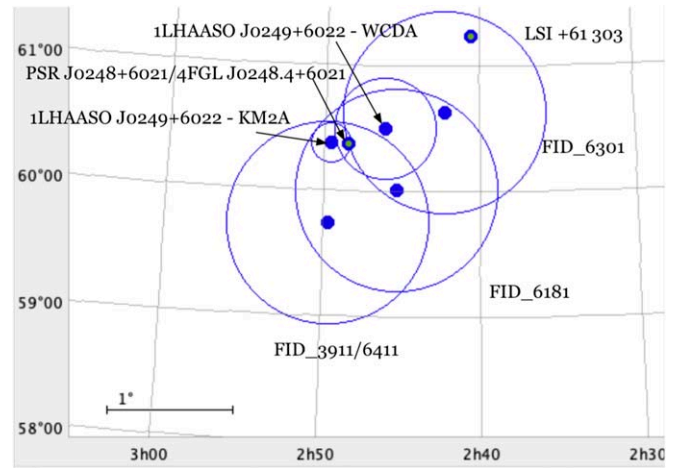


Figure 4. FAVA flare positions and $R_{95\%}$ along with LHAASO source positions and statistical $R_{95\%}$ that are coincident with PSR J0248+6021. Nearby 4FGL sources are also labeled.

flares are from PSR J2032+4127, these flares would be the first MeV (or GeV) energy flares detected by this source at week-long timescales. Overall, especially for FIDs 6012 and 6911, a more in-depth analysis is required to accurately discern the origin of these flares and determine if this pulsar environment also produces GeV flares.

4.3.3. PSR J1731–1847

PSR J1731–1847, a millisecond pulsar (msp), is spatially coincident with a single source. This millisecond pulsar is identified to be an eclipsing binary, but this effect would only delay the timed pulses on the order of fractions of a second (Bates et al. 2011). We note that the typical likelihood analysis done by FAVA to better localize this source failed to converge (and therefore giving a $R_{95\%}$ of 0.8°), and we recommend future analysis in order to identify the origin of this flare, as it could potentially be indicative of the msp interacting with its neighboring environment (i.e., a flaring PWN). If further analysis identifies this to be the origin of the flare, it would be the first gamma-ray flare reported from this millisecond pulsar’s environment.

4.3.4. Flares Coincident with Multiple Galactic Sources Not Known to Flare

There are two more flares which may have originated from a flaring PWN but are coincident with more than one nonvariable Galactic gamma-ray source. The two flares are as follows:

1. FID 3472: found spatially coincident with SNR G016.0–00.5 and SNR G016.7+00.1.
2. FID 3473: found spatially coincident with PSR J1826–1256 and SNR G018.1–00.1.

See Table 2 for additional details on these 4FGL sources and their coincident FAVA flares. We note that both of these FAVA-detected flares were detected in the same week, and within about 1.86° from one another. FID 3473 was also reported in 2FAV and was labeled as unassociated since the flare could not be firmly established to have originated from PSR J1826–1256 alone. All known Galactic sources that are spatially coincident with these flares are classified as spp,

except PSR J1826–1256 (a known pulsar; see Table 2). Since the origin of the spp sources is currently ambiguous, we will not discuss them in particular. In order to better understand the nature of these detected flares, a robust LAT analysis needs to be applied for the week these flares were detected. However, due to the presence of multiple potential PWNe, this environment could potentially host a flaring PWN.

4.4. Potential Crab-Like Pulsar Wind Nebula

Above we discussed the potential association of FAVA flares to pulsars, and possible PWNe—both of these environments could potentially mean a flaring PWN is present. Due to the flaring state of Cygnus X-3 during the weeks flares were found coincident with PSR J2032+4127, we find it likely that those flares originate from Cygnus X-3 (which is known to be variable; see Section 4.2.1). We therefore propose that four separate flaring events (FIDs 3472, 3473, 6181, and 41136), which are positionally coincident with six different Galactic gamma-ray sources, could potentially originate from a flaring PWN. None of the coincident sources are reported as variable in the 4FGL-DR4. The VI reported in the 4FGL-DR4 for SNR G016.0–00.5, SNR G016.7+00.1, PSR J1826–1256, SNR G018.1–00.1, PSR J0248+6021, and PSR J1731–1847 is 12.78, 4.00, 8.95, 14.78, 8.14, and 14.66, respectively. Since the 4FGL uses monthly binning for its light curves and this would only be a single week-long outburst at most, we find it unlikely to be detected in the 4FGL analysis. Although the follow-up likelihood analysis that is automatically done by FAVA converged (in most cases) for these flares, the $R_{95\%}$ of FIDs 3473 and 3472 are on the order of $\sim 40'$ ($< 0.8^\circ$). Detailed LAT analysis of all of these flares in their respective time windows while implementing improvements to the analysis (e.g., pulsar gating) may enable the identification of the origin of these flares.

Therefore, if any of these known gamma-ray sources are the origin of the flare, this would be the first reported gamma-ray flare reported from any of the sources. More importantly, if this flare originates from a PWN, that would make this flare the second variable PWN ever detected in gamma rays. The only other PWN known to be variable in gamma rays is the one surrounding the Crab Nebula (Bühler & Blandford 2014).

4.5. Overview of Unknown/Unassociated FAVA Flare Properties

Out of the 10 individual unassociated flaring events that survived the cuts we implemented in Section 3, two of them (FIDs 55913 and 55822) positionally overlap, likely originating from the same source. The distribution of our 10 flares on the Galactic plane is depicted in an Aitoff projection in Figure 2.

With a selection criteria of a 5σ detection in either of the photometric FAVA HE or LE bands, we find that five unassociated flares are detected exclusively in the LE band (FIDs 55913, 1281, 6101, 6631, 72921), one exclusively in the HE band (FID 57924), and four detected in both bands (FIDs 55822, 14127, 56019, and 60334). See Table 5. The follow-up likelihood analysis implemented in FAVA, with our calibration of its calculated $R_{95\%}$, gives a more accurate $R_{95\%}$ than the photometric localization method alone. Additionally, the maximum-likelihood analysis gives an estimation of the photon index of the flare in each band. The smallest $R_{95\%}$ (including our calibration) is 0.011° (FID 55822) and the largest is 0.270°

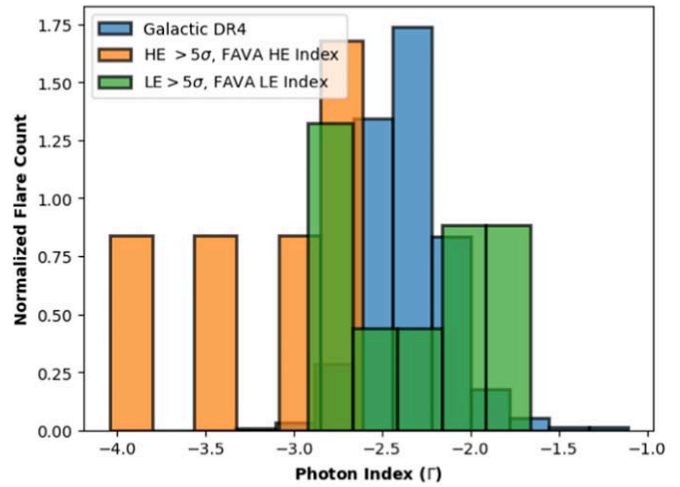


Figure 5. Distribution of power-law spectral indices from the likelihood analysis reported by FAVA for our reported unassociated Galactic flaring candidates detected in the HE band (orange) or LE band (green). This is compared with the steady-state average power-law fits for identified Galactic sources in the 4FGL-DR4 (blue). Note, most DR4 Galactic sources have their best fit with a LogParabola model but for comparison we plot the fitted power-law values.

(FID 60334), with a median value of $\sim 0.05^\circ$ across all detections. The mean photon index of all of the LE band detections ($> 5\sigma$ for LE) is -2.31 ± 0.05 (of the five detected exclusively in this band, the mean is -2.47 ± 0.08). For all the HE-detected flares, the mean photon index in this band is -3.11 ± 0.15 (FID 57924, which is detected exclusively in the HE band, has a HE index of -2.61 ± 0.34). The distribution of photon indices of the unassociated flares, compared against the fitted power-law photon index (Γ) of Galactic sources reported in the 4FGL-DR4, are presented in Figure 5.

4.5.1. Kolmogorov–Smirnov and Anderson–Darling Tests

In order to help determine if the unassociated Galactic flare candidates likely come from a source population that differs from the known Galactic or blazar sources, we implemented both Kolmogorov–Smirnov (KS) and Anderson–Darling (AD) statistical tests. Using the spectral indices calculated for the flares, we separate the flares into three subcategories: (i) flares spatially coincident with known Galactic sources, (ii) flares spatially coincident with known blazar sources, and (iii) unassociated flares. Each of these flaring source categories is then split into HE or LE detections. When there is more than one flare spatially coincident with a given source, for each energy band we use the most significantly detected flare in that band. For the unassociated subsets, we only select flares if they have a $> 5\sigma$ detection. We then run KS and AD statistical tests on all of the combinations of source subsets and energy-selected subsets.

Table 4 outlines the results of these two tests, with the p -value results of the AD test above the diagonal of 1’s with KS calculated values below. Two major takeaways should be considered. First, when testing the subsets with the LE-detected unassociated flares, for both the AD and KS tests the LE blazar flares have a higher p -value than the LE Galactic flares. In either case, the null hypothesis (unassociated sources come from a Galactic or blazar population) cannot be rejected.

Second, when tested with the HE unassociated flares, the HE Galactic flares have a higher p -value than the HE blazar flares,

Table 4
KS and AD p -value Results

	Gal. LE	Gal. HE	Blz. LE	Blz. HE	Unassoc. LE	Unassoc. HE
Gal. LE	1	...	0.407	...	0.5105	...
Gal. HE	...	1	...	0.0695	...	0.1925
Blz. LE	0.4348	...	1	...	0.7025	...
Blz. HE	...	0.04372	...	1	...	0.0125
Unassoc. LE	0.5732	...	0.7904	...	1	...
Unassoc. HE	...	0.121	...	0.009243	...	1

Note. Values are calculated with `ks.test` and `ad.test` from *R*. Values above the diagonal of 1's are the AD-calculated p -values, while below are the KS values. Only matching bands are compared.

and in both tests the HE blazars have p -values < 0.02 . This indicates that unassociated flares detected in the HE band are likely not from a blazar parent population.

4.6. Potential Counterparts of Unassociated Sources

In an effort to help identify the origin of the unassociated FAVA-detected flares reported in Table 5, we utilized multiple X-ray source catalogs (Living Swift-XRT Point Source Catalog, LSXPS; Evans et al. 2023), the Fourth XMM-Newton Serendipitous Source Catalog, Thirteenth Data Release (4XMM-DR13; Webb et al. 2020), the Chandra Source Catalog (CSC; Evans et al. 2010), and the Swift-BAT 105 month Catalog (Oh et al. 2018), as well as analyzed stacked archival data at the flare positions to determine persistent X-ray sources spatially coinciding with the FAVA-detected flare. Most of the FAVA-detected flares did not have contemporaneous X-ray data. The usage of archival X-ray data implies that we may miss the X-ray counterpart to the flares (if there was one). Therefore, all sources listed in the Appendix should only be taken as possible persistent counterparts.

In short, of the unassociated flares, three flares are coincident with 4XMM sources (FIDs 55913, 60334, and 72921), three flares are coincident with LSXPS sources (FIDs 57924, 60334, and 72921), one flare is coincident with a CSC source (FID 14127), and three flares are coincident with the Swift-BAT 105 month catalog (FIDs 14127, 55822, and 55813). We note that the coincident BAT detections are already associated to nearby blazars or the Crab Nebula. None of the persistent X-ray sources spatially coincident with one of our Galactic flaring candidates are reported to be transient in their respective catalogs. For a more in-depth description of the X-ray catalogs and the fields of each unassociated FAVA-detected Galactic candidate, please see the Appendix.

4.6.1. Flares That Lack X-Ray Data

Beyond the X-ray catalogs, the High Energy Astrophysics Science Archive Research Center (HEASARC; Nasa High Energy Astrophysics Science Archive Research Center 2014) was also searched for possible X-ray data (from Swift-XRT, XMM, Chandra, and NuSTAR) at the location of each of these FAVA-detected flares. Three of the flares detected by FAVA have no archival X-ray data from the abovementioned missions. These flares are FIDs 1281, 6631, and 6101.

5. Discussion

Due to the bright Galactic diffuse emission, as well as the systematic uncertainty, Fermi-LAT is biased against detecting flaring sources in the Galactic plane. In this work, we used 14.98 yr of data (779 weeks) to study the population of Galactic gamma-ray transients.

The 4FGL-DR4 only reports firm associations for 32 sources classified as gamma-ray binaries, novae, and PWNe. With so few known Galactic sources detected in gamma rays (we exclude millisecond pulsars in our discussion since the transient nature caused by their fast rotation is well studied), and even fewer of these source classes exhibiting transient behavior (nine as reported by Abdollahi et al. 2017), this investigation uses FAVA to identify potential Galactic candidates that would flare on week-long time periods.

After FAVA identifies flares with its photometric method, it also performs an additional likelihood analysis of the detected flares, reporting spectral properties along with a better localized position ($< 0.8^\circ$). For the unassociated flares that we posit to be Galactic flare candidates (see Table 5), of the flares detected exclusively in the HE band, the mean of the HE photon index is $\Gamma_{\text{HEavg}} = -2.40 \pm 0.28$, and of those detected exclusively in the LE band, the average LE photon index is $\Gamma_{\text{LEavg}} = -2.47 \pm 0.19$. Of the four flares detected with $> 5\sigma$ significance in both bands, their average HE index is $\Gamma_{\text{both HE}} = -3.24 \pm 0.16$ and their average LE index is $\Gamma_{\text{both LE}} = -2.11 \pm 0.05$. This seems to indicate that for these unassociated flares, when significantly detected in both bands they are generally harder in the LE band and softer in the HE band compared to the flares detected in a single energy band. Comparatively, the average photon index for a Galactic source reported in the 4FGL-DR4 is $\Gamma_{\text{Galactic 4FGL}} = -2.33 \pm 0.01$, with PWNe having the hardest average, ($\Gamma_{\text{PWNe}} = -2.08 \pm 0.02$) and novae having the softest ($\Gamma_{\text{NOV}} = -2.46 \pm 0.06$).

We draw specific attention to FIDs 1281, 6631, and 6101, as each of these flares was significantly detected and occurred at a location in the sky with absolutely no archival X-ray observations. We highly recommend that these regions be systematically searched in follow-up campaigns to identify possible counterpart candidates to the origin of the FAVA-detected flare. Although possibly coincidental, we note that each of these flares were all detected by FAVA in the LE and not the HE band (at $\geq 5\sigma$).

Table 5
Unassociated FAVA-detected Galactic Flare Candidates^a

Flare ID	R.A. (deg)	Decl. (deg)	$R_{95\%}$ ^b (deg)	LE σ ^c	HE σ ^d	LE Γ ^e	HE Γ ^f	Start Date M/D/Y	End Date M/D/Y	Closest 4FGL ^g	4FGL ^h Class	Dist/ $R_{95\%}$ ⁱ
Multiple ^j												
55822	278.46	−21.05	0.011	40.0 ^l	40.0 ^l	−2.12 ± 0.03	−2.93 ± 0.08	04/08/19	04/15/19	J1833.6–2103	FSRQ	4.1
55913 ^m	278.46	−21.05	0.024	25.8	3.7	−2.25 ± 0.04	−2.29 ± 0.87	04/15/19	04/22/19	J1833.6–2103	FSRQ	1.7
Single ^k												
1281	194.81	−65.46	0.058	7.5	1.5	−2.73 ± 0.25	−1.03 ± 0.48	01/10/11	01/17/11	J1302.9–6349	HMB	28.6
6101	138.01	−56.99	0.040	12.2	3.7	−1.66 ± 0.06	−2.98 ± 0.19	04/06/20	04/13/20	J0904.9–5734	bcu	28.2
6631	196.71	−64.75	0.169	10.2	0.6	−2.79 ± 0.16	−0.81 ± 0.48	04/12/21	04/19/21	J1302.9–6349	HMB	6.0
14127	83.69	22.01	0.014	40 ^l	10.3	−2.06 ± 0.03	−4.04 ± 0.29	04/11/11	04/18/11	J0534.5+2200	Crab Pulsar	4.1
56019	278.49	−21.1	0.019	40 ^l	40 ^l	−1.81 ± 0.03	−2.63 ± 0.07	04/22/19	04/29/19	J1833.6–2103	FSRQ	4.1
57924	135.95	−57.61	0.104	3.0	5.5	−2.52 ± 0.38	−2.61 ± 0.34	09/02/19	09/09/19	J0904.9–5734	bcu	1.42
60334	278.25	−21.36	0.270	10.7	7.4	−2.44 ± 0.2	−3.36 ± 0.57	2/17/2020	2/24/2020	J1833.6–2103	FSRQ	1.24
72921	278.43	−20.81	0.077	5.6	0.3	−2.92 ± 0.29	−1.99 ± 0.49	07/18/22	07/25/22	J1833.6–2103	FSRQ	3.3

Notes.

^a All FAVA-reported associations for these detected flares listed “None.”

^b Calibrated $R_{95\%}$ (i.e., scaled by 1.06. See Section 2).

^c Significance of detection for $E = 100\text{--}800$ MeV. The maximum possible value is 40σ .

^d Significance of detection for $E = 800\text{--}300,000$ MeV. The maximum possible value is 40σ .

^e Fitted power-law index for $E = 100\text{--}800$ MeV.

^f Fitted power-law index for $E = 800\text{--}300,000$ MeV.

^g Source in the 4FGL closest to the FAVA-detected flare by angular separation. All sources listed officially have the identifier “4FGL” prior to the listed name. All sources listed have a VI > 27.69 as reported by the 4FGL-DR4.

^h Class designations listed are reported from the 4FGL-DR3.

ⁱ Ratio of the angular separation distance between the nearest 4FGL source and the $R_{95\%}$ as reported by FAVA’s follow-up localization, rounded to the nearest tenth.

^j For clarity, the detections that likely originate from the same source are grouped together.

^k All flares listed in this section were not coincident with any other.

^l Is hitting the maximum significance threshold as reported by FAVA, and so could be higher.

^m Ratio distance <4 and Fermi LCR reports a heightened state of the nearby 4FGL source.

5.1. Estimating Flare Rates of Galactic Origin

We find 115 flares to be coincident with at least one known Galactic gamma-ray source. Additionally, we filtered the unassociated flares (as detailed in Section 3.2) to remove blazars. Our filter for selecting likely Galactic candidates is able to correctly vet blazars from our data set with an accuracy of 68.4% (based on the use of the WISE blazar strip alone). Our testing of the WISE blazar strip gave us a false-negative rate ($\text{FNR} = 100 - \text{TPR}$) of 24.3% and a false-positive rate ($\text{FPR} = 100 - \text{TNR}$) of 39.3%. Filtering flares based on sources in their $R_{95\%}$ with the WISE blazar strip resulted in 10 individual flares remaining. Based on positional coincidence, we posit that these 10 flares originate from nine distinct flaring Galactic candidates.

The false-negative rate allows us to estimate that 2–3 of our 10 unassociated flares are potentially produced by blazars. In tandem with our estimates of possible wrongful identifications (see Section 5.2), we estimate the detection of nine unassociated likely Galactic gamma-ray transients. Moreover, our false-positive rate means that we likely filter out 3–4 additional flaring Galactic candidates that were detected by FAVA.

We then estimate that over the course of the 779 weeks studied, 12–13 unassociated Galactic flares occurred. Combining these unassociated flares with the 105 FAVA flares coincident with only a single Galactic gamma-ray source as reported in the 4FGL-DR4, we estimate a total of 117–118 flaring events that are likely of Galactic origin during our time of study. If we count FAVA flares that coincide with more than one known Galactic gamma-ray source, this estimate becomes 127–128. Employing the estimate from all coincident FAVA and 4FGL-DR4 Galactic sources, along with likely Galactic candidates from this work, we estimate that there are ~ 8.5 Galactic gamma-ray transient events per year. Of those 8.5 flares, this exploration has led to the estimate that, each year, ~ 1 of those comes from an unassociated flare, ~ 1 originates from a classical nova, ~ 2 are from Cygnus X–3, ~ 2 stem from the Crab Nebula, with the other ~ 2.5 coming from other Galactic gamma-ray sources.

5.2. Likely Misidentified Detections and Most Likely Sources of Galactic Origin

Some unassociated flares fall in the vicinity of nearby 4FGL sources (typically blazars). We want to establish whether, statistically, a flare would likely be caused by a nearby variable source. We establish a “ratio distance” by taking the ratio of the distance from the flare to the nearest 4FGL source with the FAVA-reported $R_{95\%}$ (i.e., $\text{dist}/R_{95\%}$). In essence, this establishes how many σ apart the two locations are—as in, how much disagreement their positions have. If the σ is large, it means that the flare is unlikely to have originated from the nearby source. On the other hand, if the σ is small, it means that the flare potentially could have originated from that nearby source. For the purposes of identifying the most promising flares, we establish a ratio distance of ≥ 4 as the cutoff for flares that are likely not a misidentified detection of the nearby source (since their distance apart compared to their localization is large). That is, the nearby 4FGL source has a $\sim 0.006\%$ chance of being of the same origin as the detected flare based on statistical properties alone.

Furthermore, if the nearby source has a $\text{VI} > 27.69$ as reported in the 4FGL, it has $< 1\%$ chance of being a steady

source (Scargle et al. 2013; Ballet et al. 2023). Four of our FAVA-detected Galactic flare candidates reported in Table 5 are at a ratio distance of < 4 . For each of these four detected flares, the closest 4FGL source is likely variable. We suspect that these may be misidentified as new detections and are likely a flare caused by the nearby source.

Moreover, we checked these four unassociated FAVA Galactic flare candidates suspected of having originated from their nearby 4FGL source by checking the closest 4FGL source in the Fermi LCR (Abdollahi et al. 2023) using weekly time bins. FSRQ PKS 1830–211 (the closest 4FGL source to FID 55913) was flaring from a low to high state in one of its strongest flares recorded during the same week as FID 55913. For FID 57924, the nearest 4FGL source is PKS 0903–57 (a bcu) and during the week of the FAVA-detected flare this blazar is slightly above the baseline variation, but not in a distinctively flaring state. PKS 1830–211, which is also the nearest 4FGL source for FID 60334, is according to the LCR actually in a decaying state from a large flare that occurred in late December of 2019. Lastly, PKS 1830–211 (also the nearest source for FID 72921) is at a relatively stable state during the week of FID 72921’s detected flare. Overall, this leads us to believe that FID 55913 is most likely a flare originating from the blazar, but the other three (FIDs 57924, 60334, and 72921) could still potentially be from an unknown source. Therefore, we warn readers that FID 55913 is likely a flare from a blazar.

6. Summary

Outside of the large number of pulsars detected at high energies, only three other Galactic source classes are known to emit gamma rays in a transient manner: gamma-ray binaries, novae, and the Crab Nebula PWN. Of these source classes, the 4FGL-DR4 only reports persistent gamma-ray emission from 32 firmly identified sources (60 associated sources). Moreover, low statistics of Galactic gamma-ray transients for each of these source classes means the discovery of each additional Galactic gamma-ray transient adds substantially to the statistics of the source class it belongs to.

As part of utilizing FAVA to identify new Galactic gamma-ray transients, we have been able to accomplish the following:

1. Estimate a yearly Galactic gamma-ray transient rate of ~ 8.5 flares year^{-1} . The composition of this yearly rate is ~ 2 flares from the Crab Nebula, ~ 2 flares from Cygnus X–3, ~ 1 flare from a classical nova, ~ 1 unassociated source, with the remaining ~ 2.5 flares coming from other known Galactic gamma-ray sources.
2. Report the first gamma-ray flare spatially coincident with six 4FGL sources with no prior gamma-ray outbursts. These are as follows: PSR J0248+6021, PSR J1731–1847, SNR G016.0–00.5, SNR G016.7+00.1, PSR J1826–1256, and SNR G018.1–00.1. SNR G016.0–00.5, SNR G016.7+00.1, and SNR G018.1–00.1 are all classified as either a SNR or a PWN. PSR J0248+6021, PSR J1731–1847, and PSR J1826–1256 are all pulsars. If follow-up analysis confirms that the flare does originate from one of these source environments, it would potentially mean the confirmation of a flaring PWN, and possibly the discovery of the second gamma-ray variable PWN like the Crab Nebula’s PWN.
3. Determine 10 individual unassociated flares that are of likely Galactic origin.

4. Use the WISE blazar strip to filter out possible blazars based on infrared counterparts in their gamma-ray $R_{95\%}$. Furthermore, we tested the WISE blazar strip using the gamma-ray locations and $R_{95\%}$ of sources reported in the 4FGL. We report the WISE blazar strip to have a 68% accuracy rate for correctly distinguishing blazars and Galactic sources given their gamma-ray detections. We also verify that classical novae with gamma-ray emission are unlikely to be filtered out (94% are not identified as blazars).
5. Report 18 long-term flares (>1 week) from consecutive, coincident FAVA detections. These 18 long-term flares likely come from four unique Galactic gamma-ray sources. We expect at least one long-term flare per year to be detected by FAVA.
6. Potential observational confirmation of the Crab Nebula's PWN "wave" outburst behavior as predicted by Striani et al. (2011).
7. Identify spectral parameters for each unassociated flare. We find that, on average, when compared to other unassociated flares detected in a single band, unassociated flares detected significantly in both LE and HE bands tend to be harder in the LE and softer in the HE. The mean photon index for all the unassociated flares detected in the LE band is -2.34 ± 0.23 and for all unassociated flares detected in the HE band is -2.44 ± 0.43 .
8. Report (in the Appendix) persistent X-ray sources from archival data that are spatially consistent with the FAVA-detected flares. The potential Galactic flaring candidates with a persistent X-ray source coincident with their $R_{95\%}$ are FIDs 14127, 55822, 55813, 55913, 57924, 60334, and 72921.
9. Recommend fields for future X-ray study since they had no X-ray observations where a likely flare of Galactic origin was detected. These flares are FIDs 1281, 6631, and 6101.

Future follow-up and analysis of the fields with FAVA-detected gamma-ray flares of likely Galactic origin could lead to the detection of new transient sources. Most importantly, it could verify a potentially new variable PWN.

Acknowledgments

We decorously thank NASA for the generous support in funding the Fermi proposal "Studying the origin of historical Galactic transients with FAVA" (Proposal ID: 161091), which funded this research. We appreciate and thank the reviewer for the insightful comments and advice given to improve the manuscript. We graciously thank Dr. Chernyakova of Dublin City University and Dr. Dmitry Prokhorov of the University of Amsterdam for their openness to share their data with regards to the flares they studied, as well as Dr. Shaoqiang Xi, who helped with accessing the 1LHAASO catalog. This research has used the SIMBAD database, operated at CDS, Strasbourg, France. This research has made use of data and/or software provided by the High Energy Astrophysics Science Archive Research Center (HEASARC), which is a service of the Astrophysics Science Division at NASA/GSFC and the High Energy Astrophysics Division of the Smithsonian Astrophysical Observatory. This publication made use of data products from the Wide-field Infrared Survey Explorer, which is a joint project of the University of California, Los Angeles and the Jet Propulsion Laboratory/California Institute of Technology,

funded by the National Aeronautics and Space Administration. Lastly, we thank the reader for his or her interest in our work.

Software: Astropy (Astropy Collaboration et al. 2013, 2018, 2022), numpy (Harris et al. 2020), R (R Core Team 2023), SAO Image DS9 (Joye & Mandel 2003), TOPCAT (Taylor 2005), XSPEC (v12.11.1; Arnaud 1996).

Appendix A Codes

1. Code used to webscrape data from the FAVA website: DOI [10.5281/zenodo.10962864](https://doi.org/10.5281/zenodo.10962864).
2. 3D WISE blazar strip checking AllWISE sources in $R_{95\%}$ with upper limits included: DOI [10.5281/zenodo.10962762](https://doi.org/10.5281/zenodo.10962762).

Appendix B Fermi Light Curve Repository Light Curves of Known Galactic Gamma-ray Transients Detected by FAVA (Excluding Novae)

Of the sources reported in Table 2, four of them have daily, weekly, and monthly light curves generated by the Fermi LCR. These are as follows: Cygnus X-3, the Crab Nebula, PSR B1259-63, and LS I +61 303. To better understand these sources

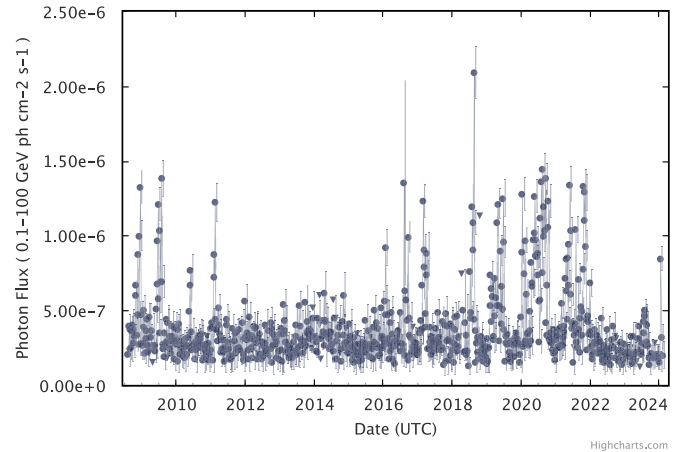


Figure 6. Fermi LCR light curve for Cygnus X-3 with weekly time binning.

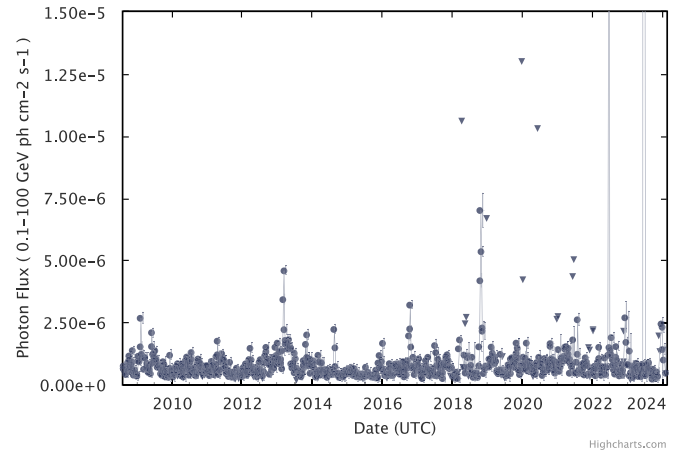


Figure 7. Zoomed-in Fermi LCR light curve with week-long time bins. One can see the smaller flares that have occurred over time. The two vertical lines near the right of the plot are flares that are almost an order of magnitude more than the Crab's typical flux value.

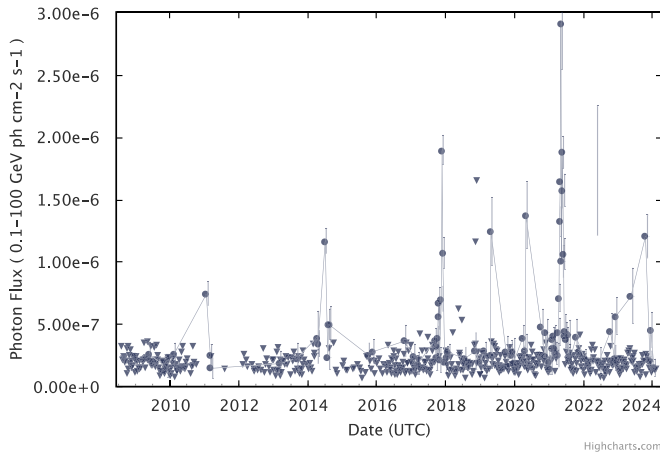


Figure 8. Fermi LCR light curve for the HMB PSR B1259-63 with weekly time binning.

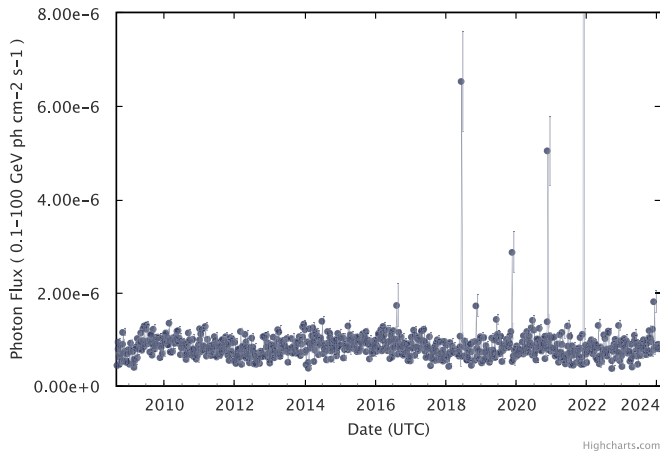


Figure 9. Long-term light curve of LS I +61 303, showing large flares around 2018, 2020, 2021, and 2022 with week-long time bins.

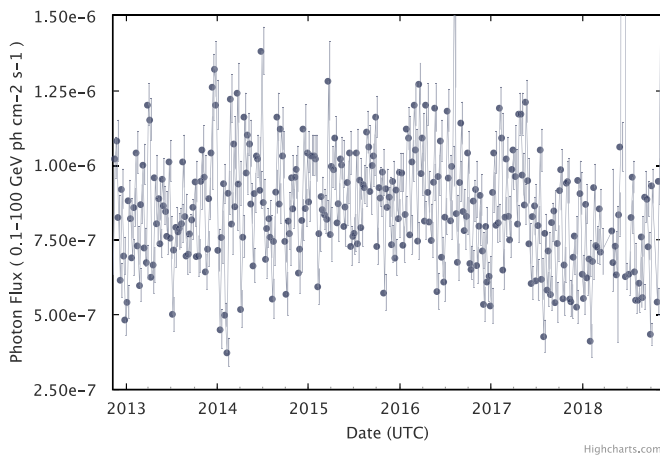


Figure 10. Shorter-term variability of LS I +61 303 with weekly time binning.

and their variable nature, we include their LCR weekly light curves in Figures 6, 7, 8, 9, and 10 for each respective source. Note, we include two for LS I +61 303, one showcasing longer-term variability (Figure 9), and one showcasing weekly variability only over a few years (Figure 10).

Appendix C X-Ray Catalog Descriptions

We cross-matched our 10 unassociated flares using the best $R_{95\%}$ from the maximum-likelihood analysis of the FAVA-detected flare with various X-ray catalogs. The catalogs are described below.

C.1. Swift-BAT 105 Month Catalog

Using $2.6'$ for Swift-BAT's, $R_{95\%}$ ¹⁵ we find three flaring Galactic candidates coincident with the Swift-BAT 105 month catalog. These are SWIFT J0534.6+2204 (the Crab Nebula) with FID 14127, and SWIFT J1833.7-2105 (PKS 1830-21) with FIDs 55822 and 55913. These cross-matches, and the other possible counterparts for each FAVA-detected Galactic flaring candidate, are discussed in detail in Appendix D.

C.2. Living Swift-XRT Point Source

The LSXPS (Evans et al. 2023) catalog updates its collection of point sources detected by Swift-XRT in real time. LSXPS covers 5371 deg^2 , and when used for this manuscript was updated through 2023 October 25. LSXPS includes a method for detecting transients. This is done by (i) determining if it is a cataloged X-ray source, and (ii) comparing the measured flux to the source's historic upper limits. See Section 4 of Evans et al. (2023) for more details. Cross-matching our FAVA-detected flares with the LSXPS transient catalog found no matches that were spatially coincident with one another. We note that a lack of X-ray monitoring over the fields of interest rather than the nontransient nature of the X-ray sources may be the cause of no cross-matches being detected.

C.3. Fourth XMM-Newton Serendipitous Source Catalog, Thirteenth Data Release

The 4XMM-DR13 (Webb et al. 2020), released 2023 June 12, includes 13,243 XMM-Newton EPIC observations from 2000 February 3 to 2022 December 31, covering over 1328 deg^2 of the sky. The 4XMM-DR13 also includes a SC_VAR_FLAG for the most variable detection of a source, SC_Fvar, which reports the lowest probability that the source is constant, and SC_chi2prob, which is the χ^2 probability that the unique source detected by one of the previous observations is constant. Out of the 54 sources that are spatially compatible with an unassociated FAVA flare, none were flagged as variable.

C.4. Chandra Source Catalog

The CSC 2.0 (Evans et al. 2010, 2020) includes 317,167 unique compact and extended X-ray sources detected by Chandra up until 2014 December 31. One of the 10 unassociated flaring Galactic source candidates are coincident with at least one Chandra detection (FID 14127).

Appendix D Possible Counterparts and X-Ray Analysis in the Field of FAVA-detected Galactic Flares

For the 10 Galactic flaring candidates, seven have archival X-ray data taken near the location of the detected event. Below,

¹⁵ See <https://heasarc.gsfc.nasa.gov/docs/heasarc/caldb/swift/docs/bat/SWIFT-BAT-CALDB-CENTROID-v2.pdf>.

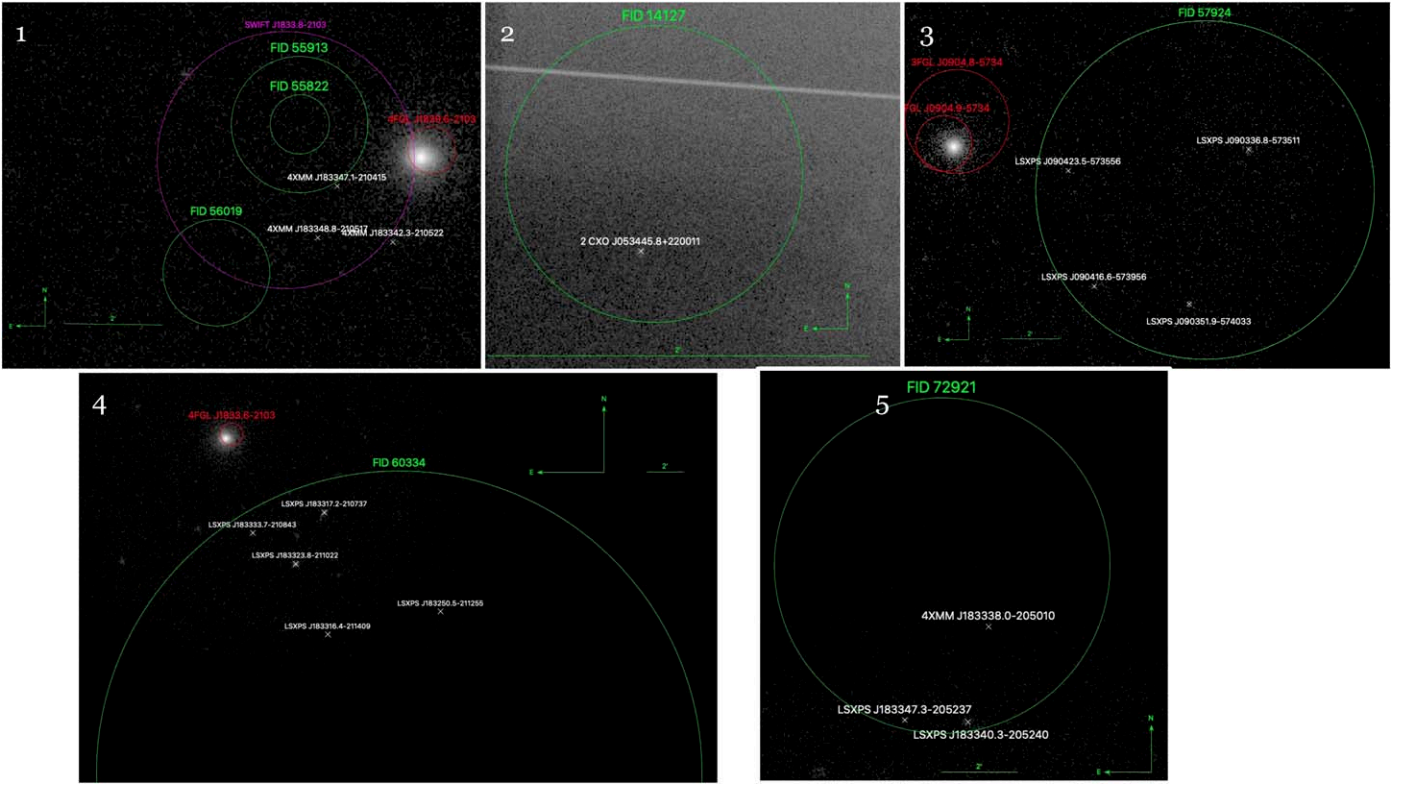


Figure 11. FAVA-detected flares with X-ray data in the same FOV are plotted here with their corresponding FAVA detection (green), nearby 4FGL sources (red), 4XMM and LSXPS survey sources (white), and Swift-BAT coincident sources (magenta). All fields were observed using Swift-XRT (with the exception of Panel 2, which was observed with Chandra). FIDs 1281, 6101, and 6631 lack X-ray data. FID 7401 is not included since it corresponds to GRB 221009A.

we outline potential counterpart candidates to the FAVA-detected Galactic flaring candidates, starting with what we find in their X-ray fields. For those lacking X-ray data, we also discuss the known sources within each flare’s $R_{95\%}$ that are reported by SIMBAD (Wenger et al. 2000). We recommend X-ray surveys of all areas of the sky covered by our flares, especially the fields that lack any X-ray observation. It is very possible that the individual counterpart responsible for the gamma-ray flare detected by FAVA is not detectable with the limited archival X-ray data we used. Since the X-ray observations do not coincide temporally with the FAVA-detected flare, these reported counterpart candidates are simply the best counterpart candidates we have available at this time.

D.1. Flare IDs 55913 and 55822

FIDs 55913 and 55822 are coincident with one another as seen in image 1 of Figure 11. The nearest 4FGL object is the FSRQ 4FGL J1833.6–2103. This variable object has been associated with the Swift-BAT detection, SWIFT J1833.8–2103, which is coincident with both flares. The ratio distance (distance to 4FGL object divided by FAVA-detected $R_{95\%}$) is 1.7σ and 4.1σ for the different flares. As discussed above, FID 55913 likely is a misidentified flare that likely originates from this blazar.

D.2. Flare ID 1281

FID 1281 is a ratio distance of 28.6σ away from the HMB 4FGL J1302.9–6379, the nearest 4FGL source, which can be completely excluded as the counterpart based on distance alone. No archival X-ray data are present for this field.

SIMBAD reports a few sources coincident with the FAVA-detected flare, including a classical Cepheid variable, a spectroscopic binary, a RR Lyrae Variable, and a couple long-period variable stars. None of these sources are convincing counterpart candidates to be the origin of a 100–800 MeV flare. We recommend future studies of this region of the sky to identify the origin of this 7.5σ LE flare.

D.3. Flare ID 6101

The nearest 4FGL source is the blazar 4FGL J0904.9–5734, at a ratio distance of 28.2σ . This large of a ratio means that this source can be excluded as the source of the flare. FID 6101 also lacks X-ray observations in its $R_{95\%}$. Searching in SIMBAD only gives stars coincident with the position of the flare. Detected with a 12.2σ significance in the LE band and 3.7σ significance in the HE band, follow-up observations are necessary to properly study the origin of this flare.

D.4. Flare ID 6631

In the neighborhood of FID 1281, FID 6631’s detected flare’s nearest known 4FGL neighbor is also 4FGL J1302.9–6379, with a ratio distance of 6.0σ . No X-ray data from Swift-XRT, XMM, or Chandra are available in the region of FID 6631. SIMBAD reports a multitude of stars of various types, but no object that would be a convincing counterpart to this significantly detected flare. Follow-up surveys of this region are required to discuss the possibilities of the origin of this flare more in depth.

D.5. Flare ID 14127

Detected on the outskirts of the Crab Nebula, FID 14127 is a ratio distance of 4.13σ to the pulsar at the center of the Crab's position (see Figure 11, image 2). The ratio distance to the nearest point in the Crab's nebula (as detected in X-rays) is 2.24σ . The FAVA-detected flare occurs well outside of the Crab Nebula itself. Checking the Fermi LCR (which only reports the nebula's synchrotron component), the Crab's PWN has an increase in its flux between 2011 April 8 and 15, going from $7.97 \pm 1.78 \times 10^{-7}$ to $1.74 \pm 0.17 \times 10^{-6}$ photons $\text{cm}^{-2} \text{s}^{-1}$ in the 0.1–100 GeV band. The average photon flux for the Crab PWN as reported through 2023 December 1 from the LCR is $1.26 \times 10^{-6} \pm 1.1 \times 10^{-11}$ photons $\text{cm}^{-2} \text{s}^{-1}$. Although this week is above the mean value, it is not a dramatic departure. This, paired with the distance to the edge of the Crab, points to this being a potential detection of a new source.

FID 14127 has a $R_{95\%}$ that has minimal overlap with the uncertainty area of the Swift-BAT detection of the nebula (SWIFT J0534.6+2204). Within the FAVA-detected flare's $R_{95\%}$, there is a CSC source present. 2CXO J053445.8+220011 was detected on 2004 January 27 at 5.87σ (Evans et al. 2010, 2020). Although detected in 2004, no other observations of this part of the sky have been observed. Therefore, at this time the Chandra-detected X-ray source appears to be the most likely candidate for the origin of the FAVA-detected flare. We recommend further studies of this X-ray source and this field to solidly confirm the origin of this flare.

D.6. Flare ID 56019

Occurring in the same region of the sky as FIDs 55913 and 55822, FID 56019 was detected in both the HE and LE bands at a significance of 40σ (the highest value that FAVA reports). With a ratio distance of 4.1σ from the nearby source, 4FGL J1839.6–2103, FID 56019 likely originates from a uniquely different source than FIDs 55913 and 55822. No persistent X-ray sources were spatially coincident with this detection

D.7. Flare ID 57924

The $R_{95\%}$ of FID 57924 does not overlap with, but is nearby to, 4FGL J0904.9–5734, the highly variable (VI = 8488.27) BL Lac object, although it was not flaring during the week of this FAVA-detected flare. The ratio of distance to the nearest 4FGL source divided by the FAVA $R_{95\%}$ is 1.42. This flare has four LSXPS sources spatially coincident with its position (see Figure 11, image 3).

Searching HEASARC, this flare has both archival Swift-XRT and Chandra data in the neighborhood of the flare. For the Chandra observation, we find the detected flares to be outside of the field of view (FOV). The most significant detection from the LSXPS J090336.8–573511, which is coincident with FID 57924, has a signal-to-noise ratio (S/N) of $S/N = 5.5$. LSXPS J090351.9–574033 was detected at $S/N = 3.9$.

D.8. Flare ID 60334





With the largest $R_{95\%}$ out of the unassociated flares, the distance to the nearest 4FGL source divided by the $R_{95\%}$ is only 1.24. The nearest 4FGL source is the FSRQ, 4FGL J1833.6–2103. This 4FGL source has a variability of 37330 reported in the DR4, but is not varying during the week of the flare.

Only part of the $R_{95\%}$ of FID 60334 has X-ray data with a number of LSXPS point sources (see Figure 11, image 4). Since only a small portion of the $R_{95\%}$ area has been observed, it is hard to determine if there is a proper persistent X-ray counterpart. This flare has 41 spatially coincident 4XMM sources and 15 LSXPS sources.

D.9. Flare ID 72921

The closest detected 4FGL source to this flare is 4FGL J1833.6–2103 at a ratio distance of 3.3. Falling on the outskirts of the Swift-XRT FOV, only a small portion of the FAVA $R_{95\%}$ has counts (see Figure 11, image 5). Even in this small area of the $R_{95\%}$, multiple sources from LSXPS and 4XMM-DR12 are present. Two of the detections overlap and coincide with the same source, those being LSXPS J183340.3–205240 and 4XMM J183340.2–205241. Due to the lack of observation of the entire FAVA detection, until additional observations are taken of this region these persistent X-ray sources are our only counterpart candidates. This source has four spatially coincident 4XMM sources and two from LSXPS.

ORCID iDs

S. Joffre  <https://orcid.org/0000-0001-9427-2944>
 N. Torres-Albà  <https://orcid.org/0000-0003-3638-8943>
 M. Ajello  <https://orcid.org/0000-0002-6584-1703>
 D. Kocevski  <https://orcid.org/0000-0001-9201-4706>

References

- Abdo, A., Ackermann, M., Ajello, M., et al. 2011, *Sci*, 331, 739
 Abdo, A. A., Ackermann, M., Ajello, M., et al. 2009, *ApJL*, 701, L123
 Abdo, A. A., Ackermann, M., Ajello, M., et al. 2010b, *Sci*, 331, 739
 Abdo, A. A., Ackermann, M., Ajello, M., et al. 2010c, *ApJS*, 188, 405
 Abdo, A. A., Ackermann, M., Ajello, M., et al. 2011, *ApJL*, 736, L11
 Abdo, A. A., Ackermann, M. A. & Fermi LAT Collaboration 2010a, *Sci*, 329, 817
 Abdo, A. A., Ajello, M., Allafort, A., et al. 2013, *ApJS*, 208, 17
 Abdollahi, S., Acero, F., Ackermann, M., et al. 2020, *ApJS*, 247, 33
 Abdollahi, S., Acero, F., Baldini, L., et al. 2022, *ApJS*, 260, 53
 Abdollahi, S., Ackermann, M., Ajello, M., et al. 2017, *ApJ*, 846, 34
 Abdollahi, S., Ajello, M., Baldini, L., et al. 2023, *ApJS*, 265, 31
 Abeyssekara, A. U., Benbow, W., Bird, R., et al. 2018, *ApJL*, 867, L19
 Ackermann, M., Ajello, M., Albert, A., et al. 2013, *ApJ*, 771, 57
 Ackermann, M., Ajello, M., Albert, A., et al. 2014a, *Sci*, 345, 554
 Ackermann, M., Ajello, M., Albert, A., et al. 2014b, *Sci*, 345, 554
 Aharonian, F., Akhperjanian, A. G., Aye, K. M., et al. 2005, *A&A*, 442, 1
 Ajello, M., Arimoto, M., Axelsson, M., et al. 2019, *ApJ*, 878, 52
 Albert, A., Alfaro, R., Alvarez, C., et al. 2022, *ApJ*, 940, 141
 Arnaud, K. A. 1996, in ASP Conf. Ser. 101, Astronomical Data Analysis Software and Systems V, ed. G. H. Jacoby & J. Barnes (San Francisco, CA: ASP), 17
 Astropy Collaboration, Price-Whelan, A. M., Lim, P. L., et al. 2022, *ApJ*, 935, 167
 Astropy Collaboration, Price-Whelan, A. M., Sipőcz, B. M., et al. 2018, *AJ*, 156, 123
 Astropy Collaboration, Robitaille, T. P., Tollerud, E. J., et al. 2013, *A&A*, 558, A33
 Atwood, W. B., Abdo, A. A., Ackermann, M., et al. 2009, *ApJ*, 697, 1071
 Aydi, E., Sokolovsky, K., Chomiuk, L., et al. 2020, *NatAs*, 4, 776
 Balbo, M., Walter, R., Ferrigno, C., & Bordas, P. 2011, *A&A*, 527, L4
 Baldini, L., Ballet, J., Bastieri, D., et al. 2021, *ApJS*, 256, 13
 Ballet, J., Bruel, P., Burnett, T. H., Lott, B. & The Fermi-LAT collaboration 2023, arXiv:2307.12546
 Bates, S. D., Bailes, M., Bhat, N. D. R., et al. 2011, *MNRAS*, 416, 2455
 Bigongiari, C. 2005, in Proc. of the Int. Europhysics Conf. on High Energy Physics, HEP2005, 20
 Brill, A. 2023, Self-Supervised Learning for Modeling Gamma-ray Variability in Blazars., arXiv:2302.07700
 Buehler, R., Scargle, J. D., Blandford, R. D., et al. 2012, *ApJ*, 749, 26

- Bühler, R., & Blandford, R. 2014, *RPPH*, **77**, 066901
- Burns, E., Svinkin, D., Fenimore, E., et al. 2023, *ApJL*, **946**, L31
- Caliandro, G. A., Cheung, C. C., Li, J., et al. 2015, *ApJ*, **811**, 68
- Cao, Z., Aharonian, F., An, Q., et al. 2024, *ApJS*, **271**, 25
- Chang, Z., Zhang, S., Chen, Y.-P., et al. 2018, *RAA*, **18**, 152
- Chernyakova, M., Malyshev, D., van Soelen, B., et al. 2021, *Univ*, **7**, 242
- Cheung, C. C., Glanzman, T., & Hill, A. B. 2012a, *ATel*, **4284**, 1
- Cheung, C. C., Hays, E., Venters, T., Donato, D., & Corbet, R. H. D. 2012b, *ATel*, **4224**, 1
- Cheung, C. C., Jean, P., Shore, S. N., et al. 2016, *ApJ*, **826**, 142
- CHIME/FRB Collaboration, Amiri, M., Andersen, B. C., et al. 2021, *ApJS*, **257**, 59
- Ciprini, S. & Fermi-LAT Collaboration 2012, in AIP Conf. Ser. 1505, High Energy Gamma-Ray Astronomy: 5th International Meeting on High Energy Gamma-Ray Astronomy, ed. F. A. Aharonian, W. Hofmann, & F. M. Rieger (Melville, NY: AIP), **697**
- Collaboration, L. 2015, *ApJS*, **218**, 23
- Cutini, S., Bernard, D., & Valverd, J. 2023, *ATel*, **15995**, 1
- Dinesh, A., Valverde, J., & Garrappa, S. 2023, *ATel*, **15925**, 1
- Evans, I. N., Primini, F. A., Glotfelty, K. J., et al. 2010, *ApJS*, **189**, 37
- Evans, I. N., Primini, F. A., Miller, J. B., et al. 2020, AAS Meeting, **235**, 154.05
- Evans, P. A., Page, K. L., Beardmore, A. P., et al. 2023, *MNRAS*, **518**, 174
- Fermi LAT Collaboration, Abdo, A. A., Ackermann, M., et al. 2009, *Sci*, **326**, 1512
- Franckowiak, A., Jean, P., Wood, M., Cheung, C. C., & Buson, S. 2018, *A&A*, **609**, A120
- Harris, C., Millman, K., van der Walt, S., et al. 2020, *Natur*, **585**, 357
- Hays, E., Cheung, T., & Ciprini, S. 2013, *ATel*, **5302**, 1
- H. E. S. S. Collaboration, Abdalla, H., Adam, R., et al. 2020, *A&A*, **633**, A102
- Ho, W. C. G., Ng, C. Y., Lyne, A. G., et al. 2017, *MNRAS*, **464**, 1211
- Holder, J., Atkins, R., Badran, H., et al. 2006, *APh*, **25**, 391
- Johnson, T. J., Wood, K. S., Kerr, M., et al. 2018, *ApJ*, **863**, 27
- Joye, W. A., & Mandel, E. 2003, in ASP Conf. Ser. 295, Astronomical Data Analysis Software and Systems XII, ed. H. E. Payne, R. I. Jedrzejewski, & R. N. Hook (San Francisco, CA: ASP), **489**
- Koljonen, K. I. I., & Maccarone, T. J. 2017, *MNRAS*, **472**, 2181
- Krimm, H. A., Holland, S. T., Corbet, R. H. D., et al. 2013, *ApJS*, **209**, 14
- Lesage, S., Veres, P., Briggs, M. S., et al. 2023, *ApJL*, **952**, L42
- Li, K.-L., & Chomiuk, L. 2016, *ATel*, **9699**, 1
- Li, K.-L., Chomiuk, L., & Strader, J. 2016, *ATel*, **9736**, 1
- Li, K. L., Kong, A. K. H., Tam, P. H. T., et al. 2017a, *ApJ*, **843**, 85
- Li, K.-L., Metzger, B. D., Chomiuk, L., et al. 2017b, *NatAs*, **1**, 697
- Li, K. L., Takata, J., Ng, C. W., et al. 2018, *ApJ*, **857**, 123
- Lien, A., Sakamoto, T., Barthelmy, S. D., et al. 2016, *ApJ*, **829**, 7
- Massaro, E., Maselli, A., Leto, C., et al. 2015, *Ap&SS*, **357**, 75
- Massaro, F., D'Abrusco, R., Tosti, G., et al. 2012, *ApJ*, **750**, 138
- Metzger, B. D., Caprioli, D., Vurm, I., et al. 2016, *MNRAS*, **457**, 1786
- Minkowski, R. 1942, *ApJ*, **96**, 199
- Mirabel, I. 2012, *Sci*, **335**, 175
- Munari, U., Hamsch, F. J., & Frigo, A. 2017, *MNRAS*, **469**, 4341
- Nasa High Energy Astrophysics Science Archive Research Center 2014, HEASoft: Unified Release of FTOOLS and XANADU, Astrophysics Source Code Library, ascl:1408.004
- Nelson, T., Mukai, K., Li, K.-L., et al. 2019, *ApJ*, **872**, 86
- Nolan, P. L., Abdo, A. A., Ackermann, M., et al. 2012, *ApJS*, **199**, 31
- Oh, K., Koss, M., Markwardt, C. B., et al. 2018, *ApJS*, **235**, 4
- Otero-Santos, J., Peñil, P., Acosta-Pulido, J. A., et al. 2023, *MNRAS*, **518**, 5788
- Peñil, P., Ajello, M., Buson, S., et al. 2022, arXiv:2211.01894
- Pittori, C., Tavani, M., Bulgarelli, A., et al. 2023, *ATel*, **15952**, 1
- Prokhorov, D. A., & Moraghan, A. 2022, *MNRAS*, **519**, 2680
- R Core Team 2023, R: A Language and Environment for Statistical Computing, R Foundation for Statistical Computing, Vienna, Austria, <https://www.R-project.org/>
- Scargle, J. D., Norris, J. P., Jackson, B., & Chiang, J. 2013, *ApJ*, **764**, 167
- Striani, E., Tavani, M., Piano, G., et al. 2011, *ApJL*, **741**, L5
- Striani, E., Tavani, M., Vittorini, V., et al. 2013, *ApJ*, **765**, 52
- Suvorov, A. G., & Glampedakis, K. 2022, *ApJ*, **940**, 128
- Tam, P. H. T., He, X. B., Pal, P. S., & Cui, Y. 2018, *ApJ*, **862**, 165
- Tam, P. H. T., Huang, R. H. H., Takata, J., et al. 2011, *ApJL*, **736**, L10
- Tavani, M., Bulgarelli, A., Vittorini, V., et al. 2011, *Sci*, **331**, 736
- Taylor, M. B. 2005, in ASP Conf. Ser. 347, Astronomical Data Analysis Software and Systems XIV, ed. P. Shopbell, M. Britton, & R. Ebert (San Francisco, CA: ASP), **29**
- Theureau, G., Parent, D., Cognard, I., et al. 2011, *A&A*, **525**, A94
- Torres, D. F., Rea, N., Esposito, P., et al. 2011, *ApJ*, **744**, 106
- Urry, M. 1999, in ASP Conf. Ser. 159, BL Lac Phenomenon, ed. L. O. Takalo & A. Sillanpää (San Francisco, CA: ASP), **3**
- van Kerkwijk, M. H., Charles, P. A., Geballe, T. R., et al. 1992, *Natur*, **355**, 703
- von Kienlin, A., Meegan, C. A., Paciesas, W. S., et al. 2020, *ApJ*, **893**, 46
- Wang, N., Johnston, S., & Manchester, R. N. 2004, *MNRAS*, **351**, 599
- Webb, N. A., Coriat, M., Traulsen, I., et al. 2020, *A&A*, **641**, A136
- Wenger, M., Ochsenbein, F., Egret, D., et al. 2000, *A&AS*, **143**, 9